Australian Government
Forest and Wood Products Research and Development Corporation

MARKET KNOWLEDGE & DEVELOPMENT

PROJECT NUMBER: PN04.2005

Maximising impact sound resistance of timber framed floor/ ceiling systems

Volume 1

FEBRUARY 2006

FWPRDC
PO Box 69, World Trade Centre
Melbourne 8005, Victoria
T: +61 3 9614 7544 F: +61 3 9614 6822

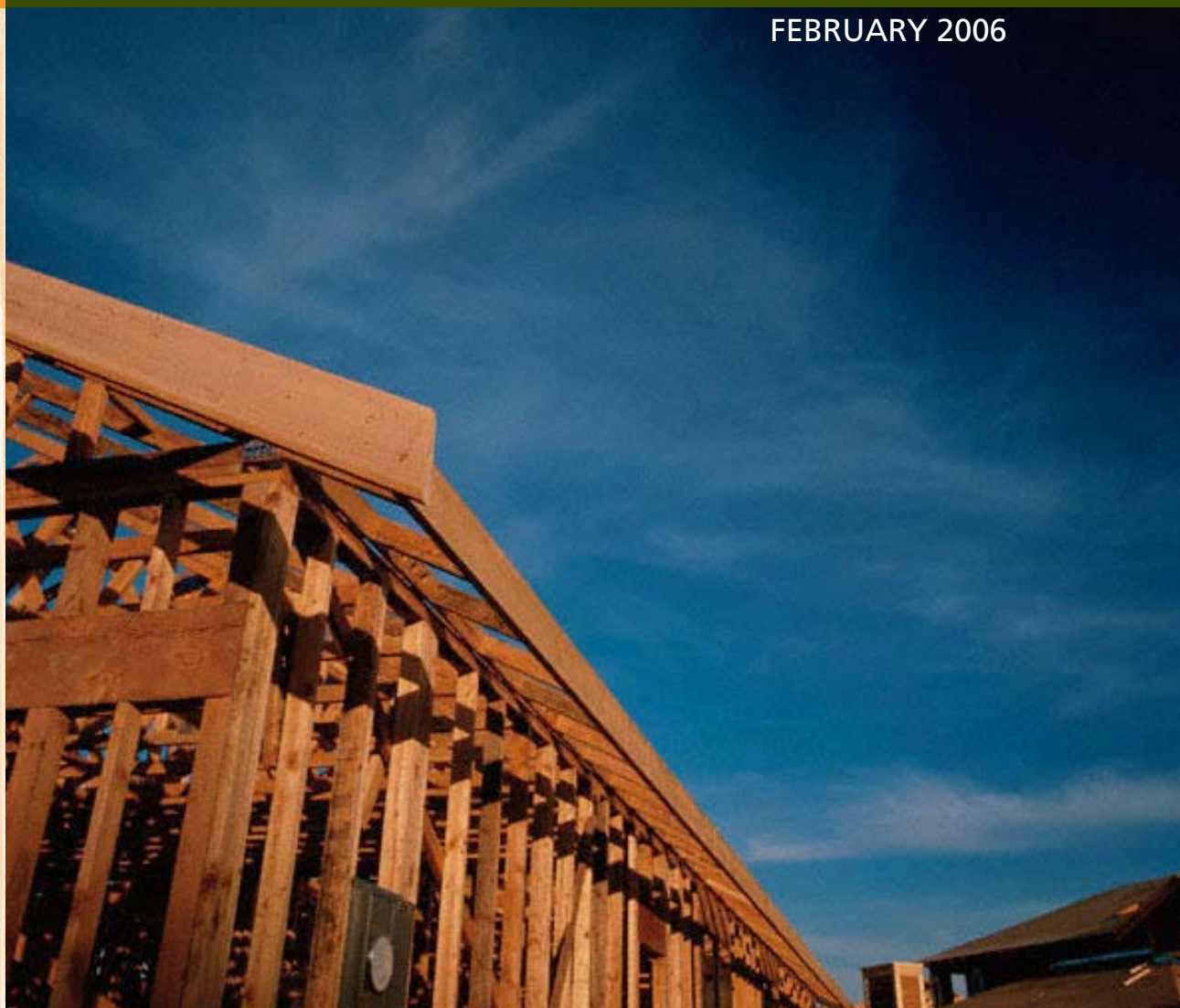

Maximising impact sound resistance of timber framed floor/ceiling systems Volume 1

Prepared for the

Forest and Wood Products Research and Development Corporation

by

H. Chung, G. Dodd, G. Emms, K. McGunnigle and G. Schmid

The FWPRDC is jointly funded by the Australian forest and wood products industry and the Australian Government.

Australian Government

Forest and Wood Products Research and Development Corporation

Publication: Maximising impact sound resistance of timber framed floor/ceiling systems

Project no: PN04.2005

Researchers:

H. Chung, G. Dodd, G. Schmid
University of Auckland
Private Bag 92019
Auckland, 1020, New Zealand

G. Emms
Scion
Private Bag 3020
Rotorua, New Zealand

K. McGunnigle
Prendos Ltd
34 Barrys Point Road
Box 33-700
Takapuna, Auckland, New Zealand

Final report received by the FWPRDC in February 2006.

Forest and Wood Products Research and Development Corporation
PO Box 69, World Trade Centre, Victoria 8005
T +61 3 9614 7544 F +61 3 9614 6822 E info@fwprdc.org.au
W www.fwprdc.org.au

EXECUTIVE SUMMARY

Current occupier perception of timber inter-tenancy floor/ceiling systems used in Australasia is that they do not perform acoustically as well as heavy masonry building systems, particularly in terms of impact sound transmission from the floor above. This perception has resulted in a limit in growth of multi-residential timber apartments in Australasia. Concern for this problem and an expectance of a growth in medium-rise apartment construction has resulted in increased Australasian research into this problem. This concern is not unique to Australasia, and as a result, a number of other countries with an interest in timber housing construction have also been researching this problem. This project essentially progressed existing Australasian and overseas research on this problem with a view to produce floor/ceiling system design recommendations for floors having acoustic properties which are comparable with concrete floor constructions, while also meeting the acoustic requirements of the Australian and New Zealand building codes, and being cost effective and buildable using existing construction industry skills.

The expected project outputs (deliverables) of the project were design recommendations for timber-based, inter-tenancy floor/ceiling systems to enable them to have an impact sound insulation performance which complies with the proposed Acoustic Regulations of the BCA and which is equal to or better than that of a 150mm concrete slab floor.

It has been found by experience from all over the world that inter-tenancy lightweight floors tend to be regarded as poor performers by occupiers in the neighbouring tenancy (usually the tenancy below). This poor performance is often expressed by occupiers as the hearing of 'bumps and thumps' from above and is due to poorer low-frequency impact insulation. As a result of this understanding the project has focussed on the issue of low-frequency impact insulation.

To achieve the project outputs the project was divided up into a number of aspects, with the focus being on low-frequency impact insulation performance:

- Theoretical modelling,
- Experimental testing,
- Subjective testing.

The theoretical modelling involved the development of an analytical model to describe the low-frequency impact insulation performance of a timber floor and the effect a room has on the sound produced by such a floor. The resulting model was novel in many respects, and will be published in international journals. The model was used to predict the performance of a timber floor when certain parametric changes were made to it. This produced a number of results and conclusions which can be used as a basis for design recommendations.

The experimental testing program involved the building and testing of 25 floor designs in a laboratory room designed for the purpose. The experimental testing consisted of low-frequency vibration measurements of the floor upper surface and the ceiling, as well as higher frequency measurements using standard procedures. The results of the low-frequency measurements were very detailed and were used to help

develop and to validate the theoretical model, as well as enabling detailed performance comparisons of the tested floors.

The subjective testing program consisted of recording the sounds made by various impacts on a selection of the experimentally tested floors. These sounds along with impact sounds from a 150mm thick concrete floor were then played back to 30 subjects in a listening room. The listening room was made to be like a living room. The subjects were asked which floor they would prefer to live with given the sounds they heard. The technique used in this procedure was a novel refinement of previous, similar subjective tests. The results of this subjective testing showed that it was possible for a timber floor to perform as well as a 150mm concrete floor. The results also showed that it was possible to correlate performance with the loudness of the impact sounds.

The results of the theoretical modelling, experiment and subjective testing produced conclusions which enabled design recommendations to be made to produce a timber floor with low-frequency performance equal to a concrete floor. The main design recommendations consisting of adding mass and vibration damping to the floor upper surface in the form of a granular material (consisting of a sand/sawdust mix), using independent ceiling joists to further insolate the ceiling from the rest of the floor, and making the ceiling heavier. These design recommendations could be used in isolation or together to produce a floor with effective low-frequency impact insulation.

PREFACE

The printed version of this report has been divided into two volumes. The first volume contains the primary discussion and analysis. The second volume contains raw results, useful diagrams and photographs. The idea is that when reading the first volume one can also refer to the second volume for relevant supporting information.

References have been divided up on a chapter by chapter basis, and are located in the final section of each chapter. These are referred to in the text by way of author surname and year of publication (if necessary).

The first chapter is a somewhat self-contained overview of the project. It is a good idea to read this chapter first, and then to refer to the indicated chapters.

Table of Contents

VOLUME 1

VOLUME 2

1 PROJECT OVERVIEW

1.1 INTRODUCTION

Current occupier perception of timber inter-tenancy floor/ceiling systems used in Australasia is that they do not perform acoustically as well as heavy masonry building systems, particularly in terms of impact sound transmission from the floor above. This perception has resulted in a limit in growth of multi-residential timber apartments in Australasia. Concern for this problem and an expectance of a growth in medium-rise apartment construction has resulted in increased Australasian research into this problem. This concern is not unique to Australasia, and as a result, a number of other countries with an interest in timber housing construction have also been researching this problem. This project essentially progressed existing Australasian and overseas research on this problem with a view to produce floor/ceiling system design recommendations for floors having acoustic properties which are comparable with concrete floor constructions, while also meeting the proposed Australian and New Zealand building code requirements, and being cost effective and buildable using existing construction industry skills.

The project outputs (project brief)

The brief for this project is encapsulated in the expected outputs (deliverables) of the project contract:
"The expected output will be design recommendations for timber-based, inter-tenancy floor/ceiling systems to enable them to have an impact sound insulation performance which complies with the proposed Acoustic Regulations of the BCA and which is equal to or better than that of a 150mm concrete slab floor."

1.2 OVERVIEW OF THE ISSUES

The aim of the project

The aim or brief of the project can be divided into two aspects:-

1) Achieving the appropriate mid to high frequency floor impact insulation performance.
2) Achieving the appropriate low-frequency floor impact insulation performance.

Aspect (1) concerns the frequency range from about 100Hz to 3150Hz, and can be reasonably well determined and rated[1] by standard impact insulation measurement techniques (e.g. following standard ISO 140) and the resulting single figure ratings (e.g. following standard ISO 717). According to the BCA Acoustic Regulations (which have subsequently come into force) a floor's mid to high-frequency performance should be such that $L_{n,w}+C_I$ is less than or equal to 62 dB. As far as almost any type of inter-tenancy floor is concerned this is relatively easily achieved by putting the appropriate resilient surface or underlay on the subfloor. It is often the case that timber floors, due to their inherently softer materials, have a head start here over concrete floors.

Aspect (2) concerns the frequency range below about 100 to 200Hz. It is in this low-frequency range that problems arise in a number of areas. For one thing, this is the area that lightweight floor systems have problems compared to heavy floor systems due to their light weight and perhaps their lower stiffness. It has been found by experience over the world that

[1] Reasonably well determined and rated means that the measurements are accurate and the resulting values, particularly the single figure ratings, are related to people's perceptions and subjective responses.

inter-tenancy lightweight floors tend to be regarded as poor performers by occupiers in the neighbouring tenancy (usually the tenancy below). This poor performance is often expressed by occupiers as the hearing of 'bumps and thumps' from above and is due to poorer low-frequency impact insulation. In part, this has presumed to have been caused by people walking or otherwise moving around on the floor above. Another contribution to these low-frequency 'bumps and thumps' can be things such as doors closing or heavier objects being dropped. On the other hand, heavy masonry systems, from experience, appear to perform 'acceptably' in this area of low-frequency impact insulation.

Another problem with low-frequency impact insulation of floors is that it is difficult to measure and rate. It is difficult to measure the low-frequency performance of a floor due to the fact that the room connected to the floor has a significant contribution to the floors' performance and it is difficult to remove this effect for low-frequencies. It is also difficult to rate the low-frequency performance of a floor because we don't really understand how objective measurements relate to people's perceptions of the low-frequency impact insulation of a floor.

Due to the uncertainty surrounding how one can express and rate low-frequency performance, and because of the appreciation that heavy masonry floors seem to perform acceptably in the minds of occupiers, the measure of acceptable low-frequency performance is to make such performance comparable to a 150mm dense concrete slab floor (as stated in the objective).

Note that in the above paragraphs on low-frequency floor performance, only lightweight floors were mentioned, rather that lightweight timber floors specifically. This is simply because the problem is not specific to timber floors, and is suffered by other lightweight systems, even thin, lightweight or hollow-core concrete slabs.

Both low and high frequency aspects of impact insulation are important. However, the problem of low-frequency impact insulation is the one which is most challenging to solve for lightweight floor systems, and hence will received the most attention in this project. This is not to say that the high-frequency impact insulation of a floor is not important, but it is something which is relatively easy to deal with and measure, having received much attention from researchers and industry.

Summary of the Problems

The problem of the impact insulation performance of floors can be divided into a number of factors which influence the overall result; these are illustrated in Figure 1-1.

The first factor is the impact source itself. The issue here is knowing which impact sources represent activities that happen in apartments, or at least, ultimately produce a result which ranks floors according to the occupiers' opinions.

The second factor is the reaction of the floor to impact forces imposed on it. The reaction we are primarily concerned with is how the ceiling of the floor vibrates in response to the impact forces. The issue here is to produce floor designs which minimise the ceiling vibrations which produce offending sounds for the impacts that typically occur in apartments.

The third factor is the influence of the room on the sound generated by the ceiling vibrations. It is important to realise that the so-called receiving room itself is a highly influential factor in sounds that are produced by the ceiling vibrations. This is particularly so for low-frequency sounds.

The fourth factor is the psychoacoustic response of the occupants in the receiving room below the floor. This factor is how the occupiers react to the sounds that are produced in the receiving room. This subjective aspect of the problem is important to determine how well floors and sounds generated by impacts on them perform against each other and against some reference (i.e. how they can be ranked). This is possibly the most important factor of the problem, but is also possibly the most nebulous.

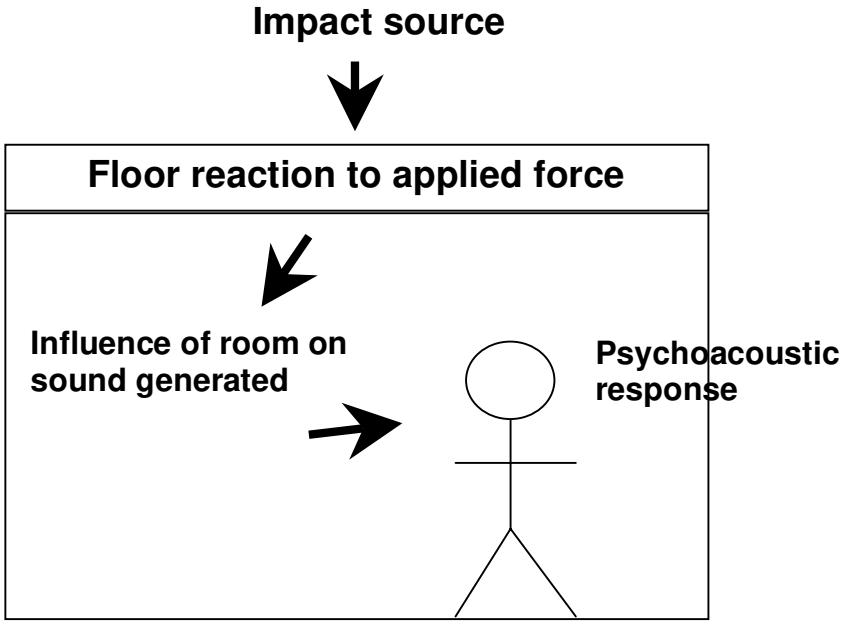

Figure 1-1. Diagram illustrating the breakdown of the problem into factors influencing the outcome.

1.3 OVERVIEW OF EXISTING KNOWLEDGE

The problem of low-frequency impact sound insulation in light-weight timber floors has been an issue for a long time. In recent years, research and anecdotal evidence have identified the problem as being of major concern for customers. In particular, the increased acceptance and use of light timber-framed construction in various parts of the world has highlighted the issues in certain countries (for example, in the US Blazier and DuPree (1994) highlighted increased customer perception of low-frequency impact sounds). As a result, a number of research projects have looked into this issue. Probably the most significant research project into this area was done in Scandinavia, by Finland, Sweden, Norway and Denmark. As part of the so-called Nordic R&D project "Multistorey timber frame buildings", the project consisted of each contributing country selecting a number of suitable floors (after some experimental development), and then installing these floors into real building developments with occupants. This project spanned 5 years and finished in 1999. A number of summary papers have been completed by the main researchers into this project, a good one being that produced by Hveem (1998), the principal researcher of this project.

Existing Low-frequency Performance understanding

The results of the Nordic R&D project resulted in a number of conclusions and desires for further work. It is worth summarising their conclusions here, because they seem to be a set of effective conclusions about the problem – echoing conclusions of other research projects. Hveem (1998) produced these conclusions:-

- There is a trend against stiffer joist construction in the form of deeper joists, i.e. the fundamental frequency shouldn't be too high. This echoed by Blazier and DuPree (1994).
- Lightweight floating floor systems (e.g. a couple of layers of particleboard on 20mm mineral wood board) don't improve impact insulation below 160Hz. Even heavyweight floating floor systems (e.g. 50mm dense concrete on 20mm mineral wool board) won't improve low-frequency performance below 50Hz, at best.

- The elastic suspended ceiling systems they used perform well, but have a resonance frequency of about 30Hz, and hence have limitations.
- Completely filling (or, even overfilling) the cavity with mineral wool has a positive effect on performance, especially for the cavity depths found in floors.
- For the low-frequency range it is important to separate the most dominating natural frequencies in the floor system from the modes in the room, given by typical dimensions.
- The peak energy of a footfall occurs in the frequencies below 50Hz.

Sipari (2000), the leader of the Finnish contribution to the acoustic aspect of the Nordic R&D project, concluded that the way forward is to increase mass and stiffness of the floor and floor parts. They found in their testing that a composite floor consisting of concrete slab bound to joists, so that they structurally work together, is an effective solution. They also concluded that a floor with a mass greater than 200 kg/m^2 acts satisfactorily in most cases. This possibly presents an issue since, at such masses, floors can't be regarded as lightweight elements; bearing in mind that a dense concrete slab floor 150mm thick would be about 350kg/m^2. This would be especially of concern for seismic considerations, where we may find that different bracing schemes are required. However, Sipari (2000) also suggested that lightweight floors full of mineral wool in the airspace could be developed to satisfy occupants, based on their results; it is not said how, 'though. Sipari also produced a figure (reproduced in Figure 1-2) showing where timber floors perform poorly against concrete floors and in what frequency range certain resilient components in a floor improve performance.

In the previous summaries no comment has been made of vibration damping. Work by Walk and Keller (2001) emphasised the importance of considering vibration damping in floor performance, since they believed that a lightweight floor will not have enough mass to perform well without extra damping.

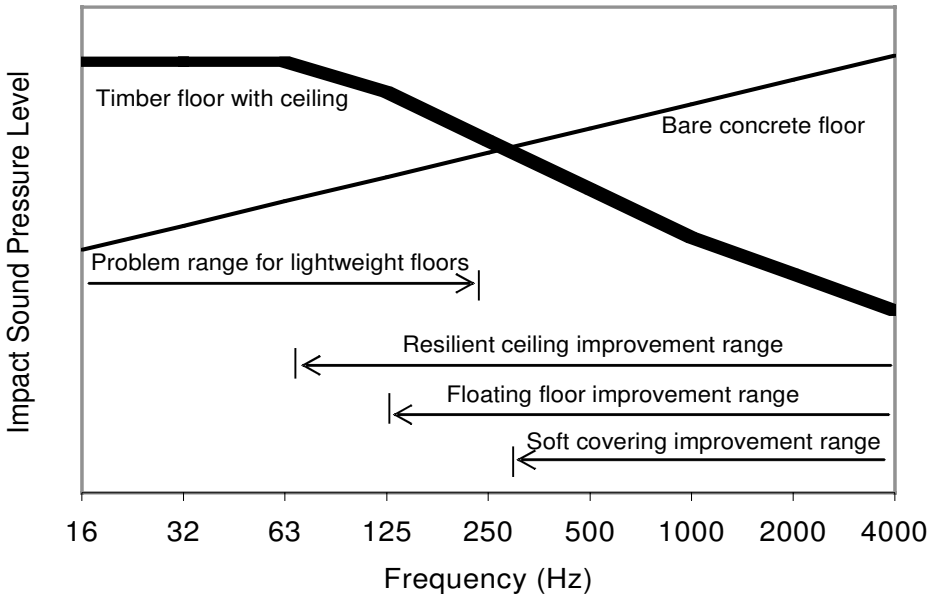

Figure 1-2. Impact sound insulation of a timber floor compared to a concrete floor and areas where certain resilient aspects of the floor design will change its performance (after P. Sipari). The soft covering and floating floor improvement range can start at lower frequencies than shown; it depends on the type of system (e.g. heavy floating floor systems or carpet on underlay can show significant improvements starting at approximately 100Hz).

Existing High-Frequency Performance understanding

Although this project is focused on improving the low-frequency performance of timber-framed floors, the high-frequency performance[2] is a critical aspect of a floors performance too. It is often the case that if there are high-frequency problems, they overshadow low-frequency issues. Having said this, it is easier to deal with high-frequency than with low-frequency problems in lightweight floor systems. One of the reasons for this is that it is easier and more meaningful to measure and rate the high-frequency impact insulation performance of a floor using standard methods, and so it has been easier to develop solutions.

In the case of lightweight timber floors, the issue of high-frequency impact (and airborne) insulation comes down to one of resilience and disconnection between masses:-

- To reduce high-frequency vibration being transmitted into the floor, the upper surface should be soft, or if hard, floating on a resilient layer.
- For vibration that has entered the floor, to prevent it from being transmitted to the ceiling and then radiated into the space below the floor, there should be good decoupling of vibration to the ceiling by use of resilient ceiling connections or separate ceiling joists mounted on resilient supports. There should also be good airborne sound decoupling between the floor and the ceiling in the form of a cavity with fibrous infill.

Guidance for reducing high-frequency impact sound transmission through lightweight floors is available in a number of text books on building acoustics. Recent work by Warnock and Birta (1998), where 190 floor systems were tested for sound insulation performance, did result in a number of observations for guidance on the matter of impact insulation of lightweight floor systems, as well as a empirical, regression-based formulation to predict the Impact Insulation Class[3] of a floor system.

As far as this project is concerned, we will only be concerned with keeping a weather eye on the high-frequency performance; in the sense of noting whether particular designs are better or worse for high-frequency impact sound insulation performance, as well as doing standard tapping machine tests on all floor systems.

This analysis of existing knowledge is extended in Chapter 2; please refer to that chapter for more information. This section only covered the broad knowledge of floor design. Further research has been done into other aspects of the project such as the subjective analysis and the theoretical modelling. The summaries of the literature available for those aspects of the project are available in their associated chapters.

1.4 THE STRUCTURE OF THE RESEARCH PROJECT

The research project was structured in order to respond to the factors influencing the problem of the low-frequency impact insulation of timber floors. With relatively minor attention being paid to the issue of the higher frequency impact insulation of timber floors. The project was divided into these three areas:-

1) Low-frequency theoretical modelling of timber floors and receiving rooms.
2) Experimental measurements of the impact insulation of floors for both low and high frequencies.
3) Subjective assessment of the floors.

Obviously these areas are not independent of each other, and the results of one area influences the progress and decisions made in other areas.

---

[2] In the context of this research project high-frequency refers to frequencies above 200Hz, and low-frequency to those below 200Hz. Strictly speaking, you might regard the frequency range above 200Hz to be mid and high frequency realm.

[3] Impact Insulation Class (or IIC) is defined in the ASTM set of standards.

Theoretical modelling

Theoretical modelling is important to enable deeper understanding of what is happening and to enable predictions without having to build numerous floors to test to produce empirical results. It also enables the testing of ideal or extreme situations to illustrate concepts. In this project a low-frequency theoretical model of a joist floor was developed, as well as a low-frequency model of a receiving room. Chapter 3 describes the development of both models.

Once developed, tested against measurement, and refined, the theoretical modelling was used to perform a trend analysis on parameters of the floors. This trend analysis is presented in Chapter 4.

Experimental measurements

A series of experimental floors were built in a laboratory and tested for both low and high frequency performance. The procedure used to test the low-frequency performance consisting of directly measuring the vibration of the floor using a shaker to excite the floor and a scanning laser vibrometer to measure the vibrations that resulted in the floor. Chapter 7 describes this procedure and contains a selection of the raw results. Standard tapping machine measurements were also made on the experimental floors; these results are contained in Chapter 8. Diagrams and photographs illustrating the design and construction of these floors are contained in Chapter 11.

Subjective analysis

As mentioned before, a critical aspect of the impact insulation performance is how occupiers might react to the sounds of impacts on various floor designs. For this subjective aspect of the project, recordings of various types of impacts were made on the experimental floors, and played back to test subjects in a listening room. The feedback from these test subjects was then used to compare a selection of the experimental floors and to give information which would allow the generation of a suitable low-frequency assessment rating system for a floor. Chapter 6 describes the subjective analysis in detail.

1.5 CONCLUSIONS OF THE ANALYSES

Theoretical Analysis Conclusions

In this section we offer some conclusions from the analysis of the theoretical model which is found in Chapter 4. These are divided into particular regions of the floor. The descriptions of the trends of the theoretical analysis relate to changes from a ‘basic’ inter-tenancy floor, illustrated in Figure 1-3.

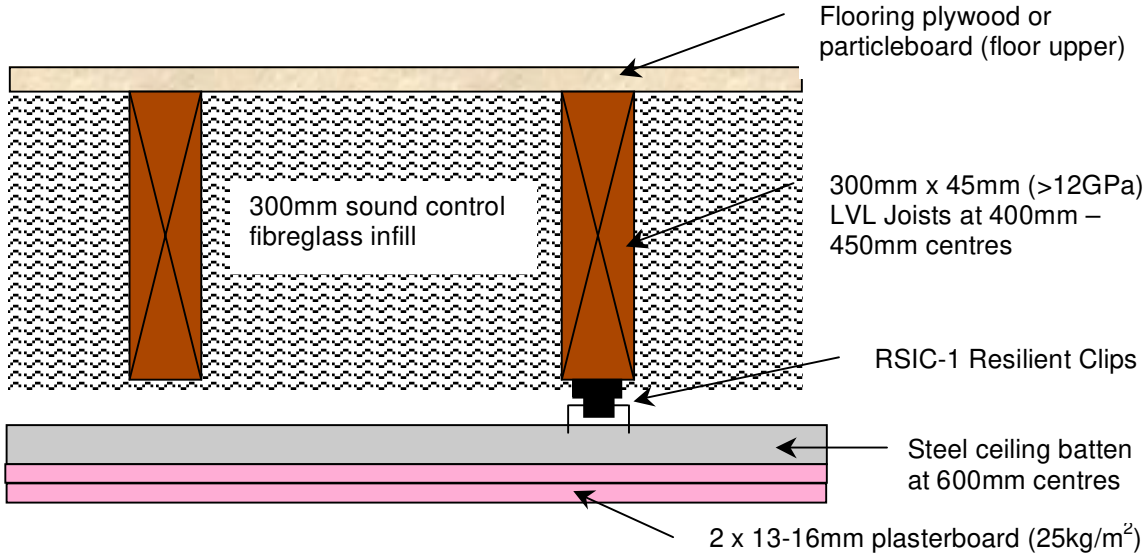

Figure 1-3. Illustration of the 'basic' inter-tenancy floor.

Joists

- It would appear that massively increasing the stiffness of the joists substantially improves performance. However, at least a four-fold increase in bending stiffness of the joists from the 'basic' floor is required for a significant gain.
- Increasing the damping of the joists does improve results by reducing the resonance peaks, especially the fundamental.
- The addition of transverse stiffeners made from blocking and tie rods can show some improvement by increasing the spacing between resonances. The improvement is not very great however, especially for wider floors where much greater transverse stiffness is required to achieve significant results. Such a feature may be best used for very narrow floors.

Floor upper (section of floor on the joists).

- It is no surprise that increasing the surface density of the floor upper does improve the performance, but after about 100kg/m^2 it would appear that minimal gains are to be had, unless unreasonable surface densities are used.
- Increasing the bending stiffness of the upper only offers slight gains.
- Increasing the damping of the upper offers some significant gains in the performance in terms of reducing the resonance peaks. However, the performance as indicated by the loudness of the low-frequency impacts is limited by the first horizontal resonance in the room. In some cases, a resonance in the floor might coincide with that in the room, and in such cases damping would be obviously beneficial.

Floor cavity

- The major conclusion from the floor cavity results is that for cavity depths greater than about 200mm the resilient rubber ceiling clips are the dominant sound transmission path. It is clear that very significant gains could be had by reducing the stiffness of the ceiling clips, or by using independent ceiling joists. However, independent ceiling joists can be prone to flanking transmission issues in a similar way to staggered stud walls.

- It is interesting to observe the effect increasing the damping of the ceiling clips has on performance. This appears to be due to the fact that, since the ceiling clips are a dominant transmission path, increasing the ceiling clip damping reduces the mass-spring-mass resonance of the floor system at around 30-40Hz. We also see an improvement in other low-frequency resonances.

Ceiling

- Increasing the surface density of the ceiling improves the performance significantly. It would seem that, for a given amount of mass in the floor system, having about half the mass on the floor upper and half in the ceiling produces best results. This result relates well to the fact that airborne sound reduction in double-leafed constructions performs best for a given amount of mass when an equal amount of mass is to be found on each leaf.
- Greatly increasing the stiffness of the ceiling can have a detrimental effect whereas increasing the damping has a positive effect. Both of these results are probably related to the fact that the dominant sound path to the ceiling is through the ceiling clips.

Floor and room dimensions

- Increasing the span of the floor tends to improve performance up to a point. In part, this effect appears to be due to the movement of the fundamental resonance along the longest length of the room to a different frequency which might start to coincide with resonances in the floor.
- Changing the width of the floor does affect the results, but produces no trend as such, apart from increasing the size of the receiving room and hence the overall sound absorption.
- Changing the height of the receiving room only changes the results above the first vertical mode of the room (at around 60-80Hz, depending on the height). As a result, there is little influence on the loudness ratings, particularly for footstep sounds, since the energy is mostly concentrated below 80Hz.

Experimental Analysis Conclusions

In this section the conclusions from the experimental impact insulation results are presented. More detail can be found in Chapter 5.

Low-frequency conclusions

The conclusions drawn from the low-frequency testing on the floors tend to be the same as those found in the theoretical model analysis, although what was experimentally tested was a subset of the analysis that could be done theoretically.
In summary, the conclusions are:-

- The addition of transverse stiffeners did show the ability to reduce the density of resonance frequencies in the low frequency region.
- The addition of mass and stiffness in the floor upper improves low-frequency performance.
- The addition of damping in the floor upper improves low-frequency performance.
- The use of a sand/sawdust mix as an infill in a battened cavity in the floor upper provides good results, by way of adding mass, adding a lot more damping, and adding some floor upper stiffness.
- Extra ceiling layers improve low-frequency performance.
- Independent ceiling joists can improve the low-frequency performance if care is taken to isolate them and the ceiling from vibration from the edge of the floor. This shows

that the ceiling clips (even the rubber RSIC clips used) are the dominant sound transmission path. When care was not taken to isolate the ceiling joists and the ceiling, they performed as well as the RSIC clips.

High-frequency conclusions

Although the focus of the project was not exactly on high frequency impact insulation, we did make standard tapping machine measurements on the floors and did find some interesting results:-

- The addition of transverse stiffeners in a floor significantly improved the high-frequency impact insulation (by 5dB in the floors tested) for the case when the floor upper was thin with little stiffness (e.g. one layer of plywood).
- Extra ceiling layers did not improve the high-frequency impact insulation.
- The span of the floor did not affect the high-frequency results.

These are the more interesting conclusions from the high-frequency results, further conclusions are made in Chapter 1.

Subjective Analysis Conclusions

In Chapter 6 the subjective analysis is described. A number of timber floor designs (nine in total) were subjectively tested using impacts that consisted of a standard Japanese impact ball, walking, and the tapping machine. These timber floors were compared against a reference 150mm concrete floor with an added suspended ceiling so that it met the Australian building code ($L_{n,w} + C_I \leq 62$). One conclusion from the subjective analysis was that a floor design consisting of 85mm of sand in the floor upper, as shown in Figure 1-6, performed as well as the reference concrete floor for the low-frequency impacts (viz. the ball drop and the walking. Another conclusion was that the subjective results correlated well with loudness measures of the impact sounds, enabling such rating methods to be used for further analysis.

Buildability Conclusions

Although there is not a separate chapter on conclusions to be had about buildability, it was a topic studied by asking Australian housing developers about such things. As a result of this discussion and through the existing knowledge of members and companies of the project team, some buildability issues did come out as being important and are listed:-

- The overall depth of the floor is an issue, however, the view was expressed that it is not a critical factor: designs can be adjusted to accommodate deeper floors, if necessary. In fact, it is good to have deeper joists (300mm) to accommodate air conditioning services, and to achieve greater spans.
- The total weight of a floor is an issue, for seismic concerns in New Zealand, but a weight of about 150kg/m^2 is acceptable if standard LTF bracing systems and methods are to be used.
- The use of wet trades is an important factor. The delay and project management issues they bring to the job are very important. One major advantage of timber construction is that they lack wet trades in the construction. This would seem to rule out the use of concrete screeds.
- Cutting and laying of multiple layers of sheeting material is time consuming. To overcome this, the inter-tenancy floor for a whole tenancy could be completed and then infill walls added later.

Other Considerations

There are some other, miscellaneous considerations which are worth noting:-

- Another issue is concern about the embodied energy of a building. Timber is seen as a material with a low embodied energy (as well as being a carbon store), and other

materials used should have similar qualities, including being available locally (to reduce transportation energy requirements).

- It is important that the floor not have noticeable felt vibrations. It is often stated that this requirement is met by ensuring the fundamental frequency of the floor is above 8Hz.
- It has been observed by a number of people that a floor which feels solid is good (e.g. Pitts (2000)). People have a tendency to like concrete screeds on timber subfloors for this reason. Since subjective opinions are complicated, this could a contributing factor for reports that thick concrete screeds are effective.

1.6 SUCCESSFUL FLOOR DESIGNS

The preceding analysis has led us to develop floor designs which are deemed to be successful in the eyes of the requirements of the brief. We therefore define a successful floor to be one which, according to subjective testing we have done, has similar performance to a 150mm concrete floor. We also require that the floor be buildable with skills that exist in the market, and that there be few proprietary products in the floor system. We also would like the floor to be a dry construction to retain one major advantage of LTF construction.

Floor design A

The initial testing phase of the project and the theoretical modelling showed that a floor consisting of an upper with a deep layer of sand/sawdust mix could provide a solution. Subsequent subjective analysis showed it to be about as effective as a 150mm thick concrete floor. This tested solution design is shown in Figure 1-6. In the testing program this floor was designated 'Floor 9'. The standard tapping machine (ISO 140,717) results of this floor are $L_{n,w}$=48 dB, C_I=-2 dB, $C_{I,50\text{-}2500}$=9 dB.

The cost of this floor has been estimated by a qualified quantity surveyor to be $A 63 more per m^2 than the 'Basic floor' of Figure 1-3 for construction in Sydney or Melbourne (See Chapter 9 for more information about construction cost estimates. The depth of the floor is 504mm, and weighs 156 kg/m^2 (113 kg/m^2 for the floor upper, 25 kg/m^2 for the ceiling). The joist span of this design tested was 5.5m which gave a fundamental resonance of 14.5Hz.

Possible alterations to the shown floor design

To avoid felt vibration problems it is recommended that the fundamental frequency be above 8Hz. For vibration control, a span of 6.5m could therefore be attained with the joists used, subject to other structural considerations. The more rigorous analysis in this project may allow designers extra span depending on what limits have been applied in previous evaluations for span tables.

A joist spacing of 400mm is shown; this could be changed to 450mm, without undue effects, since such a small overall change in stiffness has an insignificant effect on results.

The floor is quite deep overall; however theoretical results do show that with the RSIC clips used, the cavity depth could be significantly less without much change to the results. The problem would be making the joists stiff enough to carry the weight. A possibility here is to re-orient the battens so that they are parallel to and on top of the less deep joists, and screw the battens into the joists resulting in a composite action.

The cavity is shown full of fibreglass infill of high flow-resistivity. Theoretical modelling has shown that with the use of RSIC clips, using less infill with less flow-resistivity makes little difference to the low-frequency performance.

The ceiling is shown as being two layers of 13mm plasterboard. The critical aspect of the ceiling for low-frequency impact performance is that it has a surface density of 25 kg/m^2; 2

layers of 16mm plasterboard with the same or greater overall surface density would be acceptable (if this were needed for fire performance).

The ceiling battens don't appear to be a critical element with the RSIC clips used; they could be replaced by different battens.

Floor 9. Upper: 1 x Plywood, battens/sand-sawdust, 1 x Plywood

SECTION FIGURE 1. **Typical section across joists**

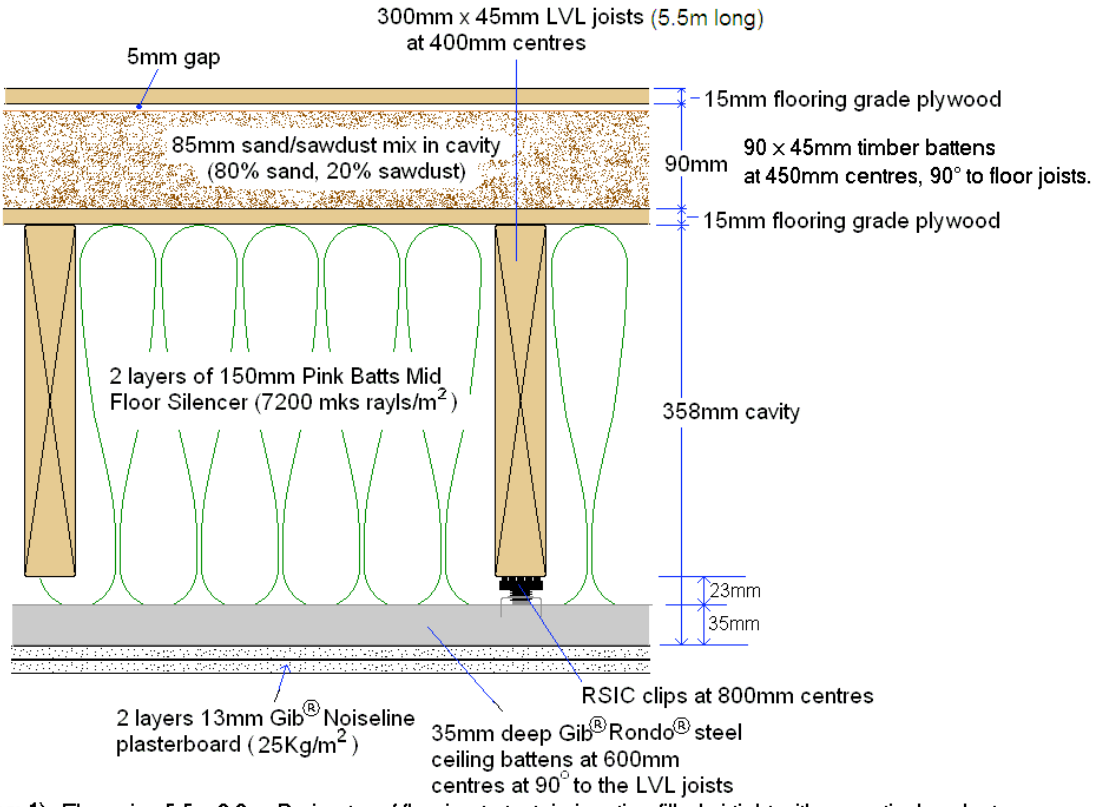

Notes: 1) Floor size 5.5 x 3.2m. Perimeter of flooring to test rig junction filled airtight with acoustical sealant.
2) One end of floor joists simply supported on 100x50mm timber grounds with solid blocking between ends of joists, other end on joist hangers off cross beam
3) For construction detail at perimeter of ceiling refer to note 3 on Floor 2, Section Figure 1

Figure 1-4. Design of floor tested in subjective testing and shown to have similar low-frequency performance to a 150mm concrete floor. (Known as Floor 9 in the experimental testing program).

Floor design B

The previous floor design (A) seemed to be an effective solution for producing a floor which is comparable to a concrete floor in performance, particularly for low-frequency performance. It does, however, use RSIC resilient clips to suspend the ceiling from the joists; whereas results from theoretical analyses did show that these clips are a major sound transmission path, even though the RSIC clips are very resilient when compared to other resilient clips or rails. There is opportunity to test a floor which uses independent ceiling joists to improve performance. However, as has been shown from experimental testing, such a system can be sensitive to how the ceiling joists are mounted, and how the ceiling edges are fixed. Nevertheless, assuming there is reasonable isolation from such flanking problems, if we use a ceiling supported by independent ceiling joists, we can expect better low-frequency performance from the ceiling system.

If we use such a ceiling with independent ceiling joists, we can then reduce the amount of material used in the floor upper. We use the same principal of adding mass and damping to the floor upper by creating a cavity filled with sand and sawdust. However, with the added performance of the ceiling system we are able to reduce the size of the battens to 70mm and hence the nominal thickness of the sand/sawdust layer to be 65mm.This floor design (which is also known as Floor 25 in the test series) is shown in Figure 1-6. The independent ceiling joists used are made of LVL to prevent distortion of the ceiling from warping of timber; it would be possible to use I-beams instead. Steel ceiling battens are fixed to the underside of the independent ceiling joists to offer a cheap, easy and stable system to fix the ceiling to. In order to prevent flanking problems, the ceiling joist ends are supported on rubber vibration isolation pads, and the ends of the battens do not connect to the wall (a separation of 10mm is used).

Floor 25. Upper: 1 x Plywood, battens / sand & sawdust, 1 x Plywood. Mid: ceiling joists: Lower: ceiling isolated.

SECTION FIGURE 1. **Typical section across joists**

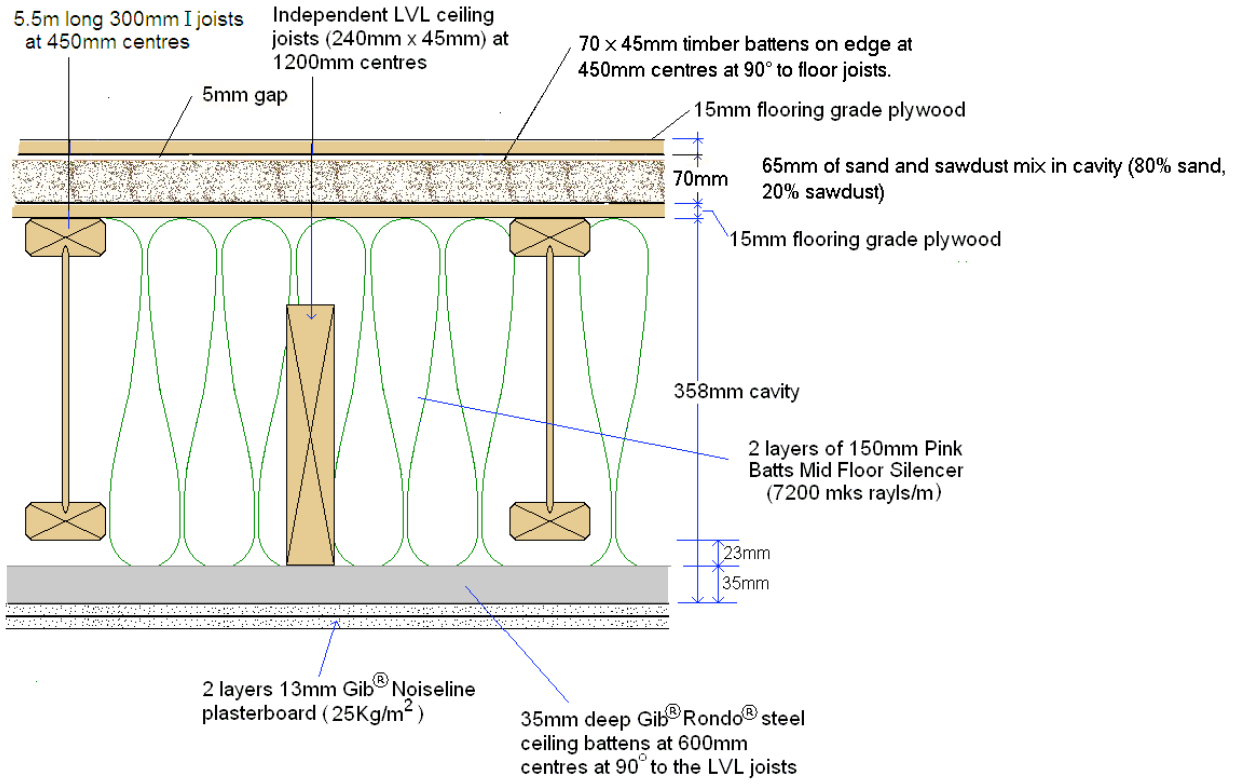

Notes: 1) Floor size 5.5 x 3.2m. Perimeter of flooring to test rig junction filled airtight with acoustical sealant.
2) One end of floor joists simply supported on 100x50mm timber grounds with solid blocking between ends of joists, other end on joist hangers off cross beam
3) Ends of ceiling joists supported on 100 x 50 x 10.5mm thick Shearflex rubber pads.
4) At perimeter of ceiling, steel ceiling battens and ceiling linings were cut to provide a 5 to 10mm gap adjacent the timber ground on the blockwork with acoustical sealant in gap.

Figure 1-5. Design 'B' of floor tested and shown to have similar low-frequency performance to floor design A. (Known as Floor 25 in the experimental testing program).

The low-frequency ceiling vibration measurements of the floor for the shaker excitation point at position 'E' are shown in Figure 1-6 with a comparison made against the results of floor design 'A' (a.k.a. Floor 9).We see from these results that the performance up to 100Hz is

about the same as floor design 'A', with a bit more variation above 100Hz. The standard tapping machine (ISO 140,717) results of this floor are $L_{n,w}$=48 dB, C_I=-2 dB, $C_{I,50\text{-}2500}$=10 dB. From these two results we can conclude that floor design 'B' has similar performance to floor design 'A', and therefore also has similar performance to a 150mm concrete floor.

The cost of this floor has been estimated by a qualified quantity surveyor to be $A61 more per m^2 than the 'Basic floor' of Figure 1-3 for construction in Sydney or Melbourne (See Chapter **Error! Reference source not found.** for more information about construction cost estimates. The depth of the floor is 484mm, and weighs 131 kg/m^2 (90 kg/m^2 for the floor upper, 25 kg/m^2 for the ceiling). The joist span of this tested design was 5.5m which gave a fundamental resonance of 13Hz.

Additional tapping machine tests were done on ceramic tiles adhered to a substrate of 10mm Gib gypsum fibreboard "Sound Barrier', which was screwed to the floor. The results of this were $L_{n,w}$=53 dB, C_I=-4 dB, $C_{I,50\text{-}2500}$=3 dB.

Possible alterations to the shown floor design

To avoid felt vibration problems it is recommended that the fundamental frequency be above 8Hz. For vibration control, a span of 6.0m could therefore be attained with the joists used, subject to other structural considerations. The more rigorous analysis in this project may allow designers extra span depending on what limits have been applied in previous evaluations for span tables.

The ceiling is shown as being two layers of 13mm plasterboard. The critical aspect of the ceiling for low-frequency impact performance is that it has a surface density of 25 kg/m^2; 2 layers of 16mm plasterboard with the same or greater overall surface density would be acceptable (if this were needed for fire performance).

The ceiling battens don't appear to be a critical element; they could be replaced by different battens.

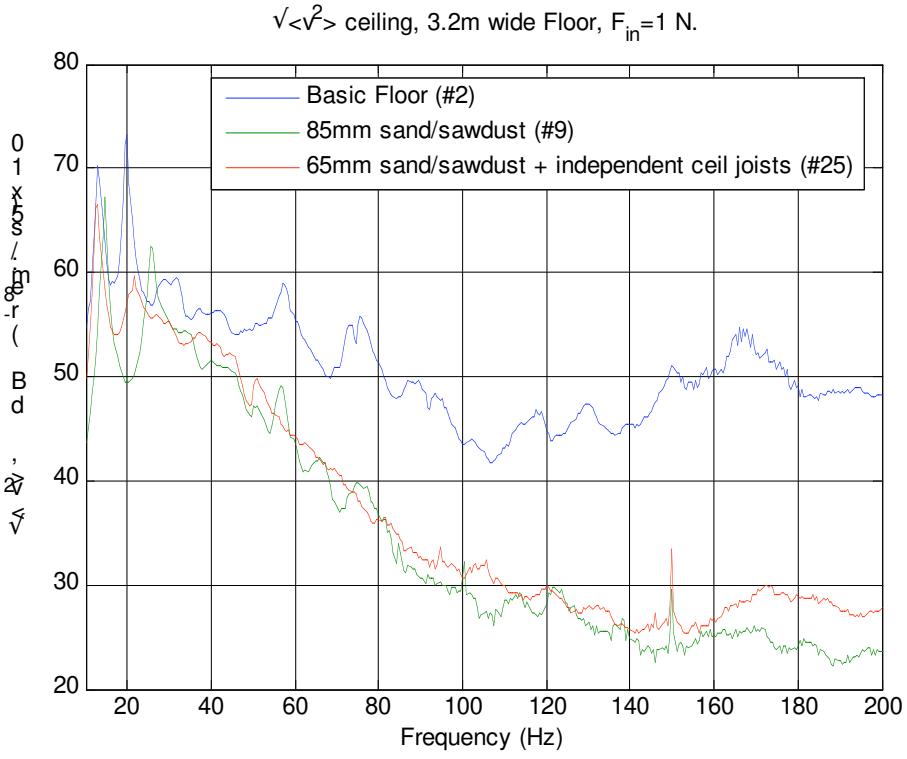

Figure 1-6. Ceiling surface average velocity results for floor design 'A' (Floor 9) as compared to floor design 'B' (Floor 25). The results for the 'basic floor' (Floor 2) are also shown for comparison.

1.7 SUGGESTIONS FOR FURTHER WORK

One of the side outputs of this project has been the theoretical model which was developed. As it stands it is in a form which is of use only to the researchers who developed it (due to the computer code it uses and its lack of an easy user interface). It is thought that this software could be useful to suitably interested and skilled people in industry. It could be adapted to make it more accessible to such people so that they can try out their own ideas and products (within the model's limitations).

1.8 TECHNOLOGY TRANSFER OF OUTPUTS

The primary channel for technology transfer and for getting systems through to the market is through our supporting companies. These companies are CSR, Winstone Wallboards, and CHH.

The results will be presented to the above companies in a face-to-face presentation. This presentation will cover the construction details of the systems and the results together with all the features, benefits, strengths and weaknesses and the actions required of the product managers in order to exploit the best possible outcomes. The purpose of the face-to-face presentation is to impart the enthusiasm, passion and commitment of the research team to the product managers. This presentation will be made available on a CD or via the internet and will be given to the supporting companies involved in the research project. Technical support will be provided by a researcher who would provide ongoing technical input over a period of up to one year. This time period would facilitate the uptake of the technology by the various company product managers to enable successful penetration into the market. Queries about the details of the features and benefits can be answered quickly and directly by the people who undertook the research work. To ensure successful implementation and transfer of the technology, additional results, photographs, etc. will be provided, if required, as part of the ongoing technical support to product managers.

The companies supporting the research project have a strong marketing capability and have been very successful in the promotion of new innovation and componentry in the field of noise control. Therefore, provided the presentation to the product managers of these respective companies is clear and timely and fills the marketing personnel with enthusiasm, then the implementation of this new technology should be carried out with due diligence and corresponding market growth. Communication of this new technology will utilise the existing marketing teams within the respective supporting companies, with support to the product managers and product development teams being sustained over a period of one year in order to clarify, confirm, expand and provide further details as and when required by the respective supporting companies.

To communicate results to FWPRDC levy-payers and key stakeholders a document will be made available for distribution to these groups summarising the results, recommended designs and benefits, and possibly suggesting how timber producers may be able to take advantage of this information. Part of this communication can be a presentation to a meeting of the Timber Association Network in Sydney, as part of the technology transfer project on MRTFC run by the TDA.

1.9 REFERENCES

Blazier, W.E, DuPree, R. B. (1994). “Investigation of low-frequency footfall noise in wood-frame, multifamily building construction”, *The Journal of the Acoustical Society of America*, 96(3), 521-1532

Hveem, S. (1998). “Comparison of low frequency impact sound insulation of different Nordic lightweight floor constructions”, *Proceedings of Acoustic Performance of Medium-rise Timber Buildings*, Dublin, Ireland, Dec. 1998.

Pitts, G. (2000). *Acoustic Performance of party floors and walls in timber framed buildings*, TRADA Technology report 1/2000.

Sipari, P. (2000). “Sound Insulation of Multi-Storey Houses – A Summary of Finnish Impact Sound Results”, *Building Acoustics*, 7(1), 15-30.

Walk, M. & Keller, B. (2001). “Highly sound –insulating wooden floor system with granular filling”, *Proceedings of ICA* 2001.

Warnock, A.C.C., Birta, J. A., (1998). “Summary report for consortium on fire resistance and sound insulation of floors: sound transmission class and impact insulation class results”, NRC-CNRC Report IRC-IR-766.

2 OVERVIEW OF EXISTING FLOOR SYSTEM DESIGNS AND RECENT RESEARCH RESULTS

2.1 INTRODUCTION

The problem of low-frequency impact sound insulation in light-weight timber floors has been an issue for a long time. In recent years, research and anecdotal evidence have identified the problem as being of major concern for customers. In particular, the increased acceptance and use of light timber-framed construction in various parts of the world has highlighted the issues in certain countries (for example, in the US Blazier and DuPree (1994) highlighted increased customer perception of low-frequency impact sounds). As a result, a number of research projects have looked into this issue. Probably the most significant research project into this area was done in Scandinavia, by Finland, Sweden, Norway and Denmark. As part of the so-called Nordic R&D project "Multistorey timber frame buildings", the project consisted of each contributing country selecting a number of suitable floors (after some experimental development), and then installing these floors into real building developments with occupants. This project spanned 5 years and finished in 1999. A number of summary papers have been completed by the main researchers into this project, a good one being that produced by Hveem (1998), the principal researcher of this project.

2.2 EXISTING LOW-FREQUENCY PERFORMANCE UNDERSTANDING

The results of the Nordic R&D project resulted in a number of conclusions and desires for further work. It is worth summarising their conclusions here, because they seem to be a set of effective conclusions about the problem – echoing conclusions of other research projects. Hveem (1998) produced these conclusions:-

- There is trend against stiffer joist construction in the form of deeper joists, i.e. the fundamental frequency shouldn't be too high. This echoed by Blazier and DuPree (1994).
- Lightweight floating floor systems (e.g. a couple of layers of particleboard on 20mm mineral wood board) don't improve impact insulation below 160Hz. Even heavyweight floating floor systems (e.g. 50mm dense concrete on 20mm mineral wool board) won't improve low-frequency performance below 50Hz, at best.
- The elastic suspended ceiling systems they used perform well, but have a resonance frequency of about 30Hz, and hence have limitations.
- Completely filling (or, even overfilling) the cavity with mineral wool has a positive effect on performance, especially for the cavity depths found in floors.
- For the low-frequency range it is important to separate the most dominating natural frequencies in the floor system from the modes in the room, given by typical dimensions.
- The peak energy of a footfall occurs in the frequencies below 50Hz.

Sipari (2000), the leader of the Finnish contribution to the acoustic aspect of the Nordic R&D project, concluded that the way forward is to increase mass and stiffness of the floor and floor parts. They found in their testing that a composite floor consisting of concrete slab bound to joists, so that they structurally work together, is an effective solution. They also concluded that a floor with a mass greater than 200 kg/m^2 acts satisfactorily in most cases. This possibly presents an issue since, at such masses, floors can't be regarded as lightweight elements; bearing in mind that a dense concrete slab floor 150mm thick would be about 350kg/m^2. This would be especially of concern for seismic considerations, where we may find that different

and additional bracing schemes are required. However, Sipari (2000) also suggested that lightweight floors full of mineral wool in the airspace could be developed to satisfy occupants, based on their results; it is not said how, 'though. Sipari also produced a figure (reproduced in Figure 1-2) showing where timber floors perform poorly against concrete floors and in what frequency range certain resilient components in a floor improve performance.

In the previous summaries no comment has been made of vibration damping. Work by Walk and Keller (2001) emphasised the importance of considering vibration damping in floor performance, since they believed that a lightweight floor will not have enough mass to perform well without extra damping.

It is worth noting that in some parts of Europe it is believed that there are two ways to obtain good impact insulation performance in floors: either through the use of mass in massive construction, or through the use of separation between the floor and ceiling for lighter constructions. Some are so convinced of the latter that they have regulated that a lightweight floor system must be at least 500mm deep[4] in building codes.

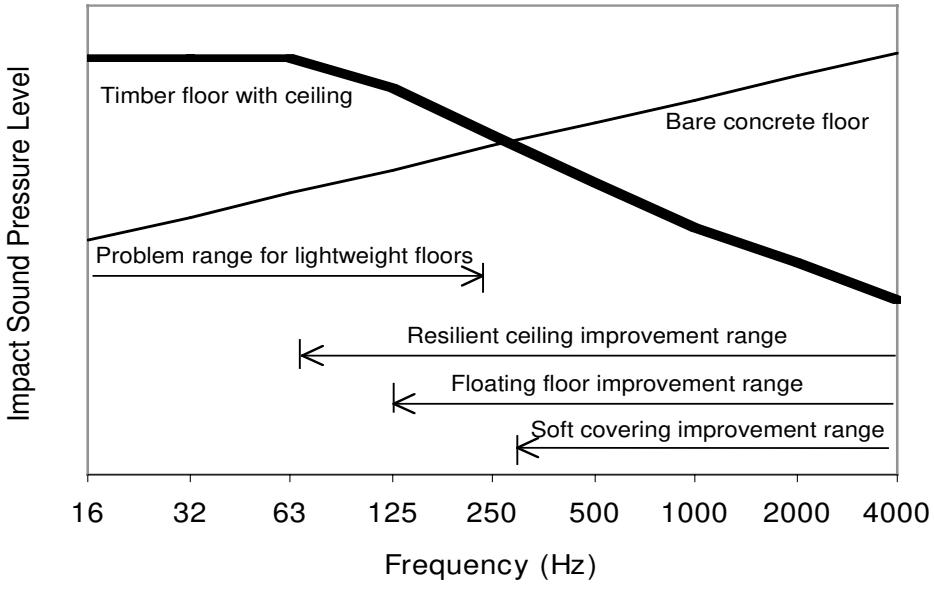

Figure 2-1. Impact sound insulation of a timber floor compared to a concrete floor (after P. Sipari).

2.3 EXISTING HIGH-FREQUENCY PERFORMANCE UNDERSTANDING

Although this project is focused on improving the low-frequency performance of timber-framed floors, the high-frequency performance[5] is a critical aspect of a floor's performance too. It is often the case that if there are high-frequency problems, they overshadow low-frequency issues. Having said this, it is easier to deal with high-frequency problems than with low-frequency problems in lightweight floor systems. One of the reasons for this is that it is easier and more meaningful to measure and rate the high-frequency impact insulation performance of a floor using standard methods, and so it has been easier to develop solutions.

[4] This was communicated to the author by Jens Rindel of DTU, Denmark.

[5] In the context of this research project high-frequency refers to frequencies above 200Hz, and low-frequency to those below 200Hz. Strictly speaking, you might regard the frequency range above 200Hz to be mid and high frequency realm.

In the case of lightweight timber floors, the issue of high-frequency impact (and airborne) insulation comes down to one of resilience and disconnection between layers of appropriate mass:-

- To reduce high-frequency vibration being transmitted into the floor, the upper surface should be soft, or if hard, floating on a resilient layer.
- For vibration that has entered the floor, to prevent it from being transmitted to the ceiling and then radiated into the space below the floor, there should be good decoupling of vibration to the ceiling by use of resilient ceiling connections or separate ceiling joists mounted on resilient supports. There should also be good airborne sound decoupling between the floor and the ceiling in the form of a cavity with fibrous infill.

Guidance for reducing high-frequency impact sound transmission through lightweight floors is available in a number of text books on building acoustics. Recent work by Warnock and Birta (1998), where 190 floor systems were tested for sound insulation performance, did result in a number of observations for guidance on the matter of impact insulation of lightweight floor systems, as well as a empirical, regression-based formulation to predict the Impact Insulation Class[6] of a floor system.

As far as this project is concerned, we will only be concerned with keeping a weather eye on the high-frequency performance; in the sense of noting whether particular designs are better or worse for high-frequency impact sound insulation performance, as well as doing standard tapping machine tests on all floor systems.

2.4 EXISTING LIGHTWEIGHT FLOOR COMPONENTS IN USE AROUND THE WORLD

Having presented a brief summary of research into the testing and design of lightweight floor systems for the improvement of impact insulation, we can now look at features of lightweight floor design which are used around the world. The particular features will be examined separately with examples of their use.

Layered upper surface floor systems

These systems consist of increasing the mass in upper part of the floor by adding layers of sheet material on to the base floor. They may or may not be placed on a resilient underlay to form a floating floor. In some cases the friction or air pumping that occurs between the layers provides extra damping.

Examples of the materials used are flooring grade plasterboard (made from alpha-gypsum), extra layers of particleboard or plywood (or similar), fibre cement sheet and gypsum fibreboard. These systems are in common use around the world where lightweight constructions are used. For example, in Scandinavia these systems, consisting of chipboard/plasterboard/chipboard layers, were common from 1987 (Hveem, 1998). They also are used in Japan, and a version consisting of two layers of gypsum fibreboard on top of the subfloor is currently promoted by USG and Winstone Wallboards in Australasia.

An example of this type of system is shown in Figure 2-2. This particular system happens to be a floating system.

[6] Impact Insulation Class (or IIC) is defined in the ASTM set of standards.

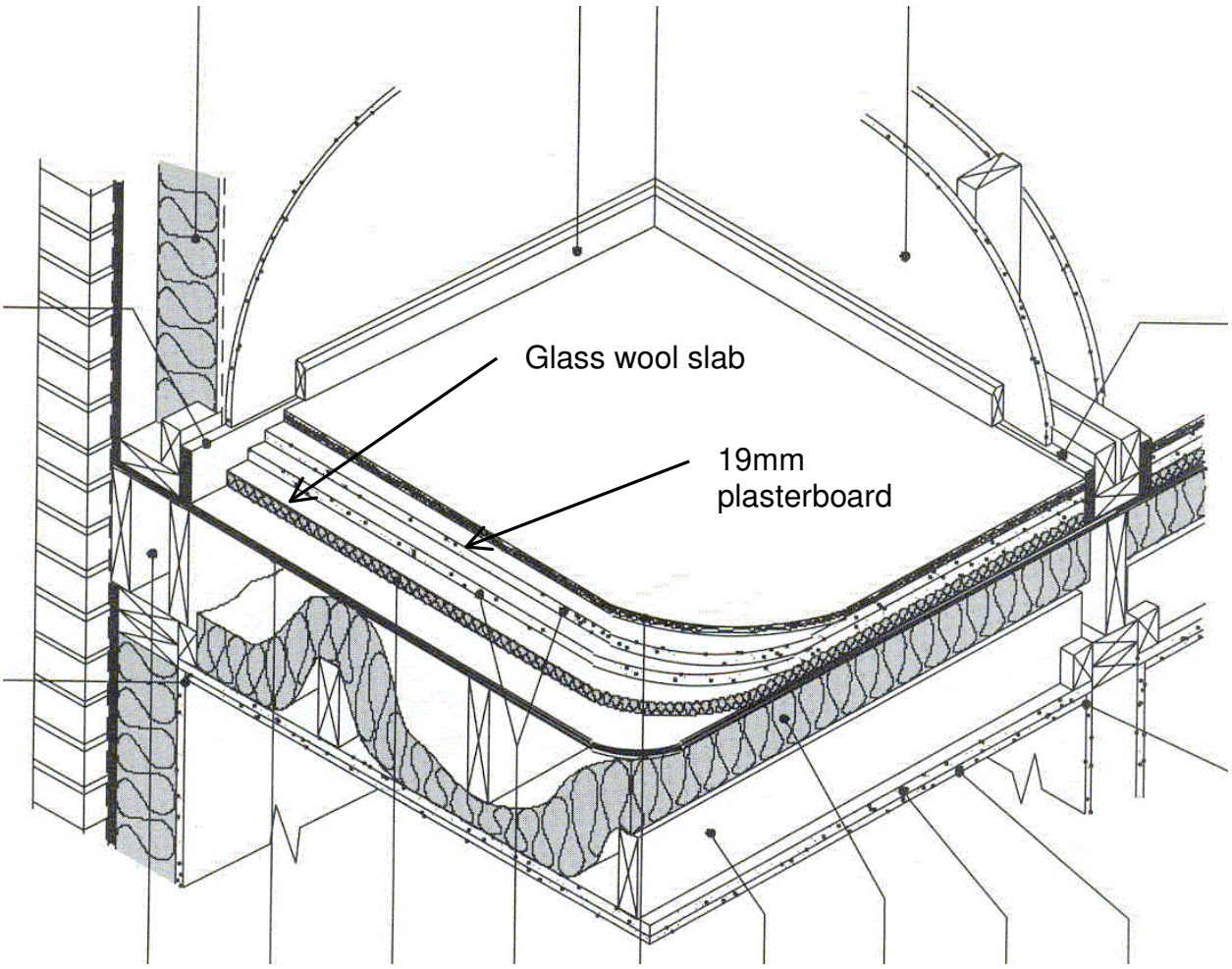

Figure 2-2. Floor design showing layered sheet material system (floating on glass wool). Also shows independent ceiling joists. (From TRADA Technology report 1/2000).

Concrete flags

In another attempt to add mass to the upper part of the floor, flags of concrete have been tried, ultimately covered with a wearing (and levelling) layer of sheet material. The flags have to be spaced by a few millimetres to prevent grinding together in service. This can be good way to get dense mass into the floor, without sacrificing dry construction advantages. These flags can be placed directly on the sub floor or floated on a resilient layer.

Screed toppings

These systems consist of some sort of concrete poured onto the subfloor. They have the advantage that they can be self levelling, and hence are also used to level the floor. They also can take heating wires for a heated floor. The screed can be poured on a resilient underlay to form a floating floor.

A common form of screed is a gypsum-based concrete, which sets quickly (in a matter of hours), allowing further building work to proceed quickly. Such gypsum concrete screeds are common in North America to the point of being almost standard practise. Gypsum concrete screeds have been trialled in parts of Europe in a floating configuration to positive effect. One trial was part of the Swedish aspect of the Nordic R&D project mentioned before and concluded that installed in a real building it proved to be more effective than layered systems in terms of occupier opinions, although lab test results may have showed the two types of systems to be have similar performance. It also has been observed by TRADA tests that the resulting surface feels good to people when they walk on it: it feels ‘solid’.

One negative side to concrete screeds is the fact that they can take some time to dry properly, even if they can set quickly. 38mm of gypsum-concrete screed can take more than 2 weeks to dry out, even in warm and well ventilated conditions. This water retention problem has resulted in occasional timber rotting issues in North America. Another negative aspect to concrete screeds is that the hard surface they present can compromise high frequency impact insulation, and so a resilient underlay is often necessary for hard, wearing surfaces. A third issue for gypsum concrete is the fact that it has to be poured quickly using specialist equipment and labour. It appears to be a specialist trade in its own right.

Composite acting floor systems

Some floor systems have an upper surface layer usually made of concrete which is directly bonded to the joists so that the upper surface and joists act together to increase stiffness. An example of this type of system has been produced by a company from Finland, Sepa Oy (Karjalainen, 2003). Figure 2-3 illustrates this particular floor design.

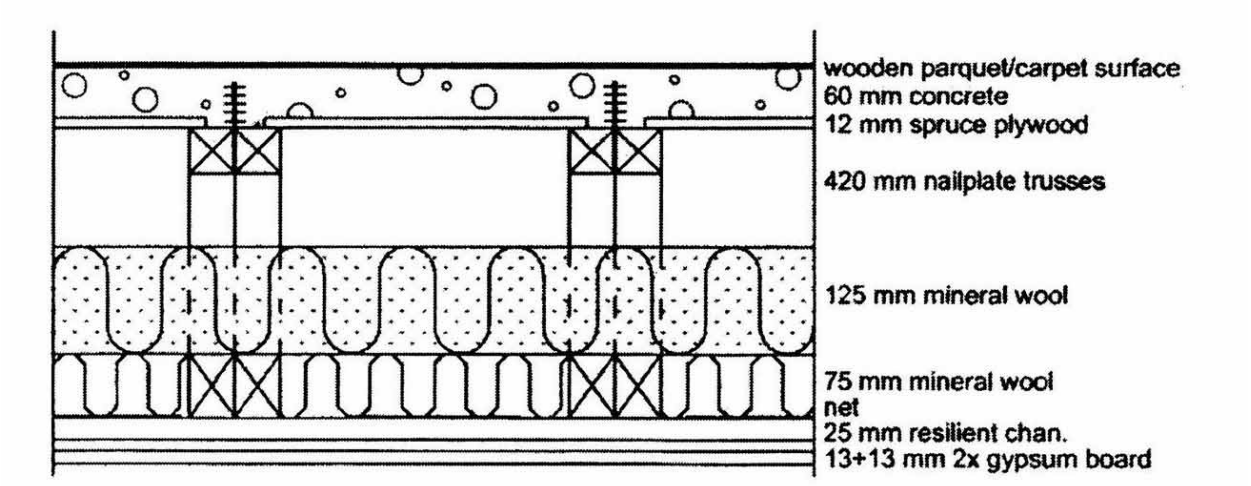

Figure 2-3. Composite wood-concrete floor system developed by Sepa Oy, Finland. Truss joists are used with the top nail plates protruding above the joist. A reinforced concrete layer is then poured over the floor. The concrete then bonds to the joists through the protruding nail plates.

Floating floor systems

In order to improve higher-frequency sound insulation, it is common to float the upper floor layer or layers on a resilient material. Usually this is only effective in reducing impact sound above 150Hz. An example of this was shown in Figure 2-2. Another common method of floating floors is to use battens which have a resilient pad on one side. There is a variant on the floating floor scheme where the subfloor has perforations in it to reduce the air stiffness in the resilient layer between the subfloor and the upper layer. An example of battens with perforations in the subfloor is shown in Figure 2-4. A problem with floating floor systems is that, in order to make then most effective, the edges must also be resiliently separated. It would appear that this can be difficult to implement consistently in practise.

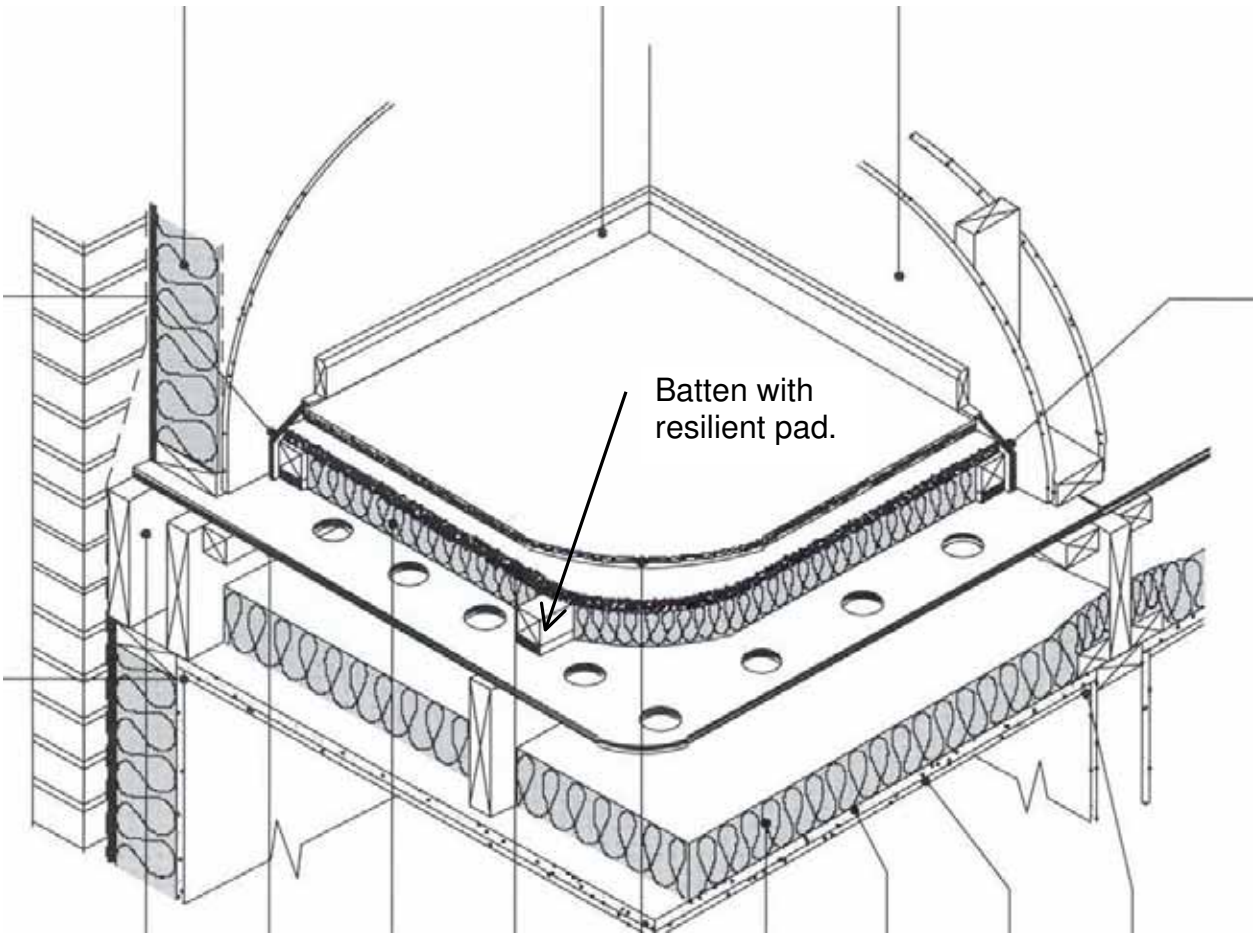

Figure 2-4. Floor system showing floating floor consisting of battens with resilient pads on one side. Also note perforations in subfloor to reduce air stiffness in floating cavity. (From TRADA Technology report 1/2000).

Resilient or disconnected ceiling systems

A lot of vibration is transmitted through the joists to the ceiling. It is better that this be isolated in some way. A common method is to use a resilient rail or channel which spans across the joists and to which the ceiling is screwed. This idea is improved by the use of rubber (or similar) ceiling batten clips which are screwed to the underside of the joists, and to which the ceiling battens are clipped. Another method to isolate the ceiling from the rest of the floor, seemingly more common in Britain, is to use separate ceiling joists to which the ceiling is screwed (as shown in Figure 2-5).

Another high-technology possibility and area of research is in the use of active noise control to control low-frequency sound for very light weight structures. Progress in this area continues, and for our problem a likely place for active noise control actuators is in the ceiling connections, where the stiffness of the air is overcome by ceiling clips with negative stiffness. An example of this sort of work is provided by Akishita et.al. (2004).

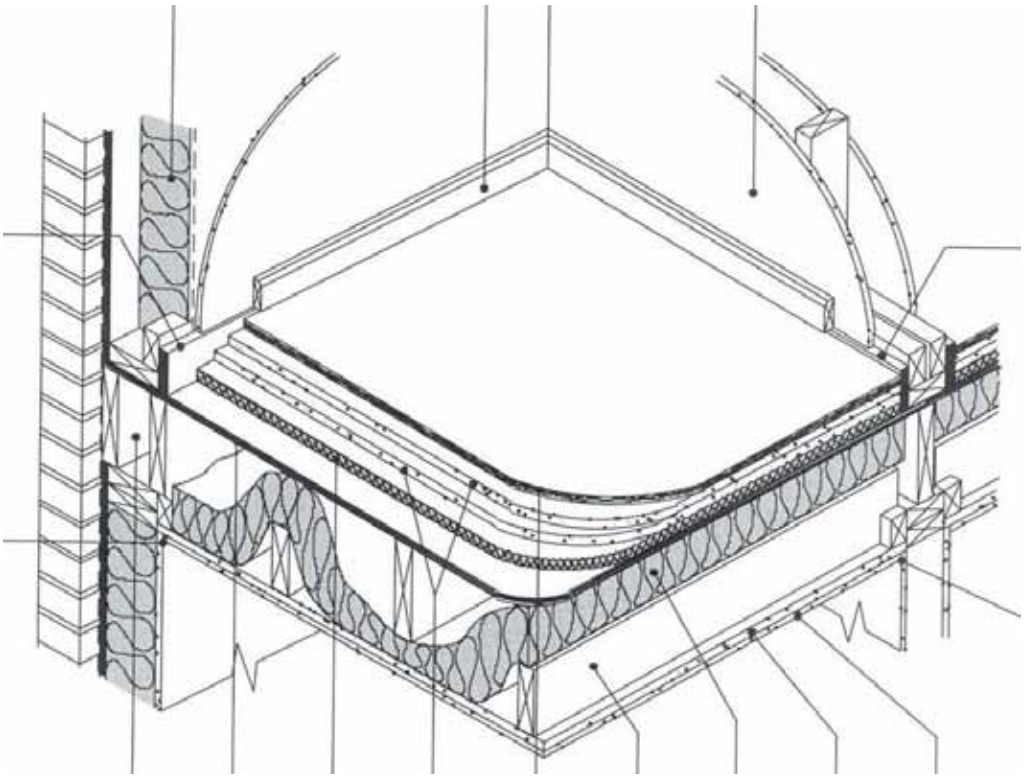

Figure 2-5. Illustration of floor with separate ceiling joists. (From TRADA Technology report 1/2000).

Raised Floor systems

Raised floor systems (access floor systems) are like those found in computer rooms and offices where there is a lot of cabling to run under the floor. They are not that commonly used around the world for floors in apartments. They are however not unusual in some parts of Japan for fitting out concrete apartments. In that situation, their main application appears to be for levelling the floor. It was noted in Japan that the opinion of occupants is that these systems increase impact noise problems of the floors, due to resonances in the air cavity (Ueda and Kakehashi, 2004).

Solid and semi-solid timber floor systems

Solid timber floors are occasionally seen in use around the world. Although it would seem to be an expensive use of timber, low-quality timber may have an application here. Recently the Swedish company Södra promoted mechanically laminated timber slab floors (from 70mm to 220mm thick) for use in multi-residential construction. It is possible that such a system could perform well in the low-frequency regime, if it were thick enough. Södra also produced a 'semi-solid' floor system made from joists spaced at 100mm centres, with the gaps filled with fibreglass. This presumably gives good stiffness (and mass) while providing a deep cavity for sound isolation to the ceiling. Such systems, however, are only worthwhile if factory made, and are probably beyond our consideration.

Granular infills

Granular or particle-type materials have been used quite frequently in the past as an infill in timber structures. It was not uncommon to have sand or fly ash in timber floors in parts of the United Kingdom many years ago – the fill would be either placed on shelves between the joists or on the ceiling (which was made of material which could support the weight). The primary function of this fill was for sound insulation purposes. Another example of this is found in some old multi-storey timber buildings in New Zealand (e.g. the old parliament buildings in

Wellington), where volcanic scoria was used in the floors. More modern references to this are found in Switzerland, where sand has been used as a layer in both retrofit and new buildings (Lappert & Geinoz, 1998). Incidentally, Lappert and Geinoz do note that the sand should be heated to ensure no living things are introduced.

Walk and Keller (2001) did recent work to develop a floor using a massive amount of 'granular' material on which a walking surface was floating. They do not say what exactly this granular material was and further communication with the authors did not reveal it, although they did say that it was being installed in a block of apartments. However, they said that the main reason for using this granular material was to take advantage of the high damping afforded by the granular material due to the friction between particles, because a lightweight floor, in their opinion, could never have enough mass to provide excellent sound insulation. Figure 2-6 illustrates this floor and shows how much granular filling there was in the floor (i.e. lots).

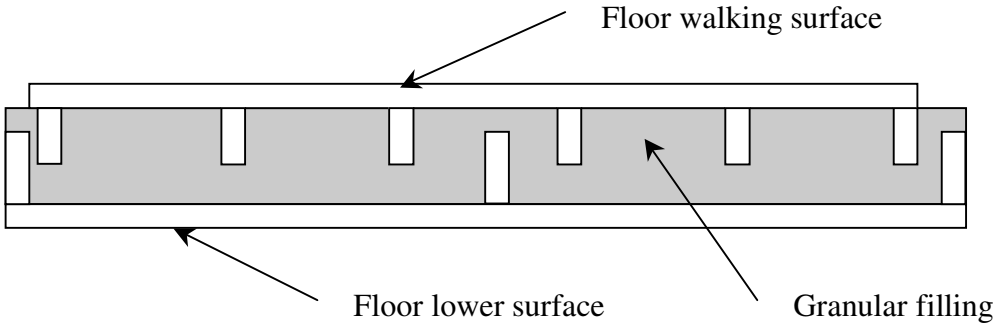

Figure 2-6. Swiss trial timber floor with upper floor surface floating on granular material (Walk and Keller, 2001).

Since granular materials, particularly sand, have been used with some success in buildings as a way of improving vibration damping, it is worth overviewing some of the literature which exists about this. It is clear from the literature that the damping processes which occur in granular materials are complicated and not very well understood apart form some specific instances.

A good account of the use of sand with other mixtures of materials has been provided by Kuhl and Kaiser (1962) for use with concrete structures. They tested various sands and mixtures (fine sand, course sand, brick rubble, and mixtures of sand and sawdust), and found that hard granular materials with sharp edges or with a soft material (e.g. sawdust or rubber dust) gave better damping at lower frequencies. They thought that this was due to the sharp edges giving more friction with vibrational strains and the lower wavespeed of vibrations in the sand sawdust or rubber dust mixtures. The sand/sawdust mixture tested was 80/20 sand/sawdust. They also note that the impedance of the granular fill should try to match the impedance of the surrounding, structural material to enable maximum coupling of energy into the granular fill. They determined that the maximum damping was attained at cavity resonances in the granular fill. The damping was also found to be non-linear in the sense that it depended on amplitude of the vibrations: higher amplitudes result in more movement of the granules and hence more friction.

Richards and Lenzi (1984) did measurements on the vibration damping due to sand and found that below a strain of 10^{-6} the particle movement is small and the damping in the sand is small and is probably not due to the friction of the particles; above that point damping becomes increasingly significant. They also noted that loose sand in cavities is useful because there is the added damping benefit of having the granules move around from regions of high density to

regions of lower density. This movement is a maximum in resonances in the cavities which contain the granular fill.

Xu et al. (2005) note that shear friction is the major contributing factor to the damping due to granular fills. Since our concern in low-frequency floor vibrations is the bending waves in the floor which would cause a lot of shearing of any infill, this is an important point to note.

Sun et al. (1986) observed from experiment that, when looking at sand laid on a vibrating metal plate, the vibrational damping in the plate is a maximum at frequencies above when the thickness of the sand is about equal to $0.05\lambda_c$, where λ_c is the longitudinal wavelength of the vibrations in the sand ($\lambda_c = c/f$, where c is the propagation speed of the vibrations (100 to 200 m/s for sand) and f is the frequency). Below this point there is a sharp drop in damping, and above this point there is a gradual decrease (due to the increasing weight of the sand packing down the sand below and stopping movement of the sand granules). Interestingly, sawdust is often mixed with sand when used for anechoic terminations for experiments with vibrations in beams. The sawdust is included to keep the sand from packing down, thereby improving its absorption characteristics.

Other damping materials

If vibration damping is important, another way to include this is to add a constrained viscous damping material, for example like a viscoelastic polymer glued between plywood layers. This can be expensive, and the polymer's damping performance can be dependent on frequency and temperature, but it is usually not dependent on vibration amplitude. Yet another way to achieve more damping is to have layers of material and to rely on the interaction between these layers to provide more damping, whether by friction between the layers, air pumping, or fretting (where the surfaces become damaged due to rubbing forming fragments thus contributing to frictional effects).

2.5 REFERENCES

Akishita, S., Mitani, A, and Takanashi, H. (2004). "Active Modular Panel Systems for Insulating Floor Impulse Noise", *Proceedings of ICA 2004*.

Blazier, W.E, DuPree, R. B. (1994). "Investigation of low-frequency footfall noise in wood-frame, multifamily building construction", *The Journal of the Acoustical Society of America*, 96(3), 521-1532

Hveem, S. (1998). "Comparison of low frequency impact sound insulation of different Nordic lightweight floor constructions", *Proceedings of Acoustic Performance of Medium-rise Timber Buildings*, Dublin, Ireland, Dec. 1998.

Karjalainen, M. (2003). "Sound insulation in Finnish multi-storey timber apartment buildings on the basis of a survey of residents", *Proceedings Wespac 8, Melbourne*.

Kuhl, W., Kaiser, H. (1962). "Absorption of structure-borne sound in building materials without and with sand-filled cavities", Acustica, 2, 179-188.

Lappert, A., Geinoz, D.,(1998). "Experience in Multi-storey timber buildings consulting and field measurement", *Proceedings of Acoustic Performance of Medium-rise Timber Buildings*, Dublin, Ireland, Dec. 1998.

Pitts, G. (2000). *Acoustic Performance of party floors and walls in timber framed buildings*, TRADA Technology report 1/2000.

Richards, E. J., Lenzi, A. (1983). "On the prediction of impact noise, VII: The structural damping of machinery", *Journal of Sound and Vibration*, 97(4), 549-586.

Sipari, P. (2000). “Sound Insulation of Multi-Storey Houses – A Summary of Finnish Impact Sound Results”, *Building Acoustics*, 7(1), 15-30.

Sun, J.C., Sun, H.B., Chow, L.C., Richards, E.J. (1986). “Predictions of total loss factors of structures, part II: Loss factors of sand-filled structure”, *Journal of Sound and Vibration*, 104(2), 243-257.

Ueda, Y. and Kakehashi, T. (2004). “A study on the relationship between bending vibration of access floor panel and floor impact sound level in an apartment building”, *Proceedings of ICA 2004*.

Walk, M. & Keller, B. (2001). “Highly sound –insulating wooden floor system with granular filling”, *Proceedings of ICA* 2001.

Warnock, A.C.C., Birta, J. A., (1998). “Summary report for consortium on fire resistance and sound insulation of floors: sound transmission class and impact insulation class results”, NRC-CNRC Report IRC-IR-766.

3 THEORETICAL MODELLING OF A JOIST FLOOR

This chapter presents a mathematical modelling of lightweight timber-based floor structures. The joist floors studied here consist of two basic components, floor upper surface, ceiling and joists. The configuration of the model is progressively made complex by adding more components in order to approximate the real structure as closely as possible. The resulting solution formulae are written into computer codes, which compute the dynamics of the structure under a given force.

This chapter is divided into three parts. The first part reviews the existing modelling methods of the LTF structures. Various articles are briefly reviewed and interrelated to each other. The second part gives the details of the floor modelling procedure, such as the Fourier expansion, composite of many components, interaction force by slippage. The third part outlines the model used to predict the sound transmission into the receiving room.

3.1 INTRODUCTION

In this chapter, we study vibration of a floor structure that has three basic components, upper plate, joist beams and ceiling. We use a mathematical modelling technique to study the dynamics of the structures. The term 'mathematical modelling' is here used for the model of the structure (LTF floor system here) using explicit formulae based on the individual material properties. In contrast, the implicit modelling uses the parameters that are derived from either the group of the structure or the whole structure. Each modelling has its advantages and disadvantages.

In recent years there have been numerous theoretical studies on the vibrations of walls, floors and ceilings, because these building components are the primary source of sounds in a room. A difficulty arises from the fact that these building components themselves are made up of many components with widely varying mechanical properties. Furthermore, the connections between different components have not been studied in detail.

There are various ways to connect the floor to the joists. We here consider simple spring model the resistance when there is slippage between the components. The amount of the resistance at the connection can be changed by varying the spring constants. We here show how the Fourier expansion method can be applied to fairly complex structures. The resulting solution is computationally efficient and robust for a wide range of physical parameters. In part II of this chapter, we will derive the differential equations that describe the upper plate and the joist beams as Kirchhof plate and Euler beams.

In part I of this chapter, various articles concerning the dynamics of the composite structures, which form a part of LTF floor system. The articles are reviewed according to their time of publication, authors and the solution techniques. The relationship between the articles is also considered.

Over the course of the project the theoretical model of the floor system was developed and refined using the experimental results from the mock-up floor structure. During the course of the research, it has been found that the interaction between the upper plat and the joist beams is crucial in determining the frequency response of the structure. The model initially had the upper plate and the joist beams. It was then made progressively complex to follow the experimental mock-up floor in realty. Eventually the model consists of the upper plate, joist

beams (for the upper plate and the ceiling), cavity air, and the sound damping filling in the cavity (glass fibre wool).

3.2 PART I: REVIEW OF EXISTING MODELS

This section introduces the papers of importance regarding theoretical modelling of wood floors. The papers are interrelated to each other. Figure 1 shows how the articles by the various researchers are related to each other. From that relationship, we may categorize the papers into three groups (Groups (a), (b) and (c)), of which two can be categorized as deterministic models and the other as empirical models.

The rule of the abbreviation is that the first two letters of the author(s) and the year of the publication are used. For example, the paper by Langley and Heron in 1990 is written as LaHe90. Additional a, b,… are used when there are more than one paper by the same author(s) in the same year. For example, Ma80a, Ma80b and Ma80c are the papers by Mace in 1980, in the order listed in References here. The most commonly used text books in all papers are Morse68, Cremer73 and Fahy85.

The series of technical reports by Hammer and Brunskog Hammer96 and Brunskog02 give detailed studies of the modelling of tapping machines and floor vibration. Their technique is based on the series of papers by Mace, Mace80, Mace80b, Mace80c, which deals with a periodically stiffened elastic plate. Mace's method is based on Mead71, Evseev73, Lin77 and Rumerman75. A few researchers in Japan have been studying the double leaf wall structure using the combination of the above two techniques, Yairi02 and Takahashi83.

In another Group of papers that deal with the transmission of vibration across a plate-beam joint, Langley90, Craik96, Craik00 are discussed. Their method is based on the techniques that are developed for laminated plates in Ashton70. The equation of motion and the force (moment) equilibrium relationship for laminated plates are derived in Ashton70. In Langley97 and Craik00a, the transmission and coupling loss factor are used in SEA to find sound transmission through a double-leaf structured walls with various connecting methods.

In Group (c), an example of an orthotropic model by Emms Emms02, Emms04 is given. The paper by Blazier and DuPree Blazier94 uses a homogeneous plate model, which uses a constant factor to convert the vibration velocity to sound pressure. The stiffness of the plate is then calculated using a generic formula based on the static elastic modulus of the individual components of the floor. For example, the physical parameters and formulae that are necessary to compute the total stiffness can be found in Australian Standards Australia93 in Appendix D.

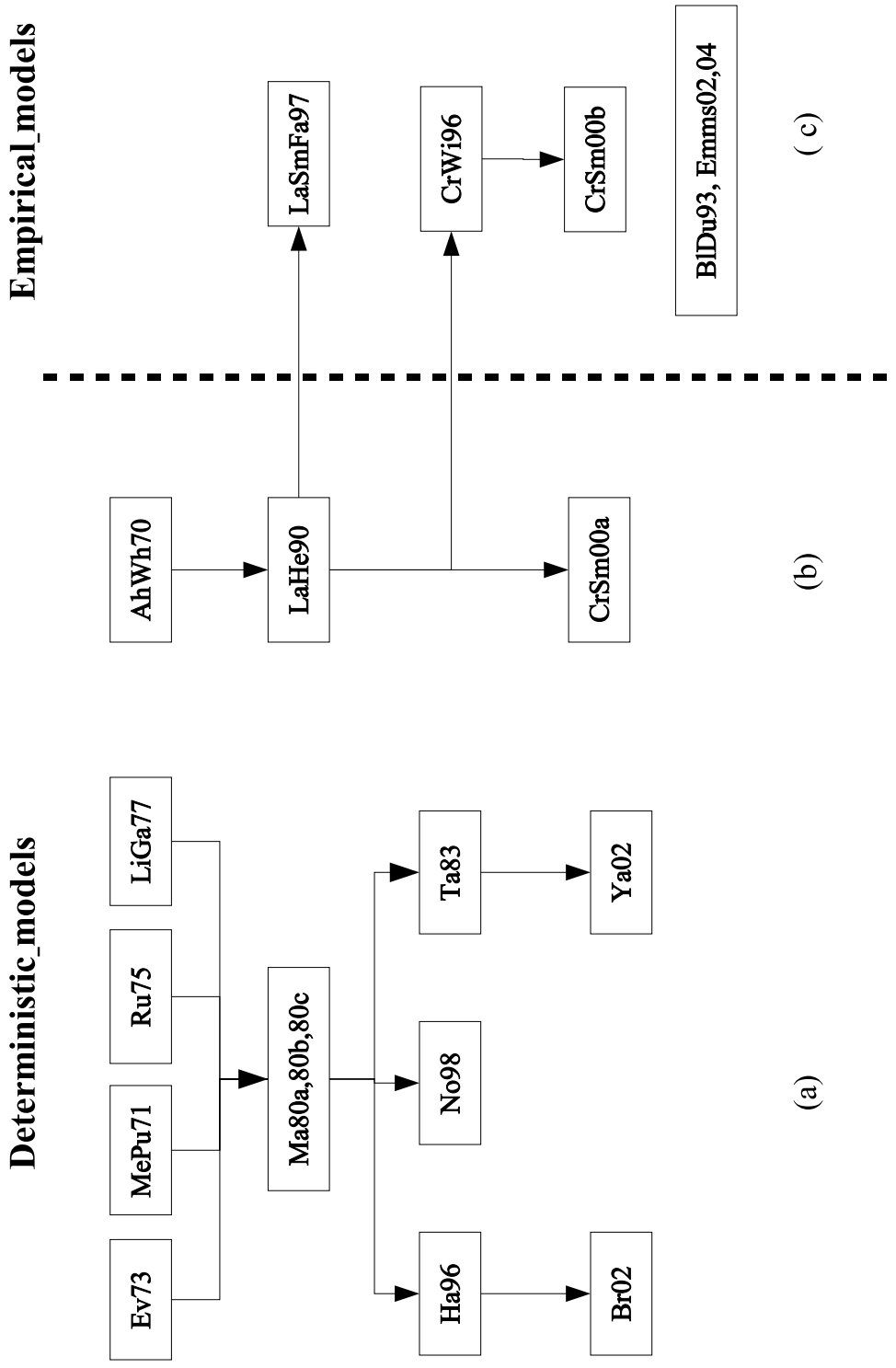

Figure 3-1: Diagram depicting the relationship between the paper.

In the following subsections, the articles by Brunskog, Craik and Emms, one from each Group in figure 3-1, will be discussed in detail because each of them represents its group well. On the left hand side of the dashed line are the deterministic models that derive explicit or approximate formulae for the deformation of the structure. On the other side are the empirical models that derive the sound pressure generated by the structure by assuming the structure is either homogeneous or orthotropic elastic plate. We however will not discuss the articles

concerning SEA in Group (c). The same notations that are used in the original papers are used when there is no confusion. Each subsection should be regarded independent from others.

Group (a)

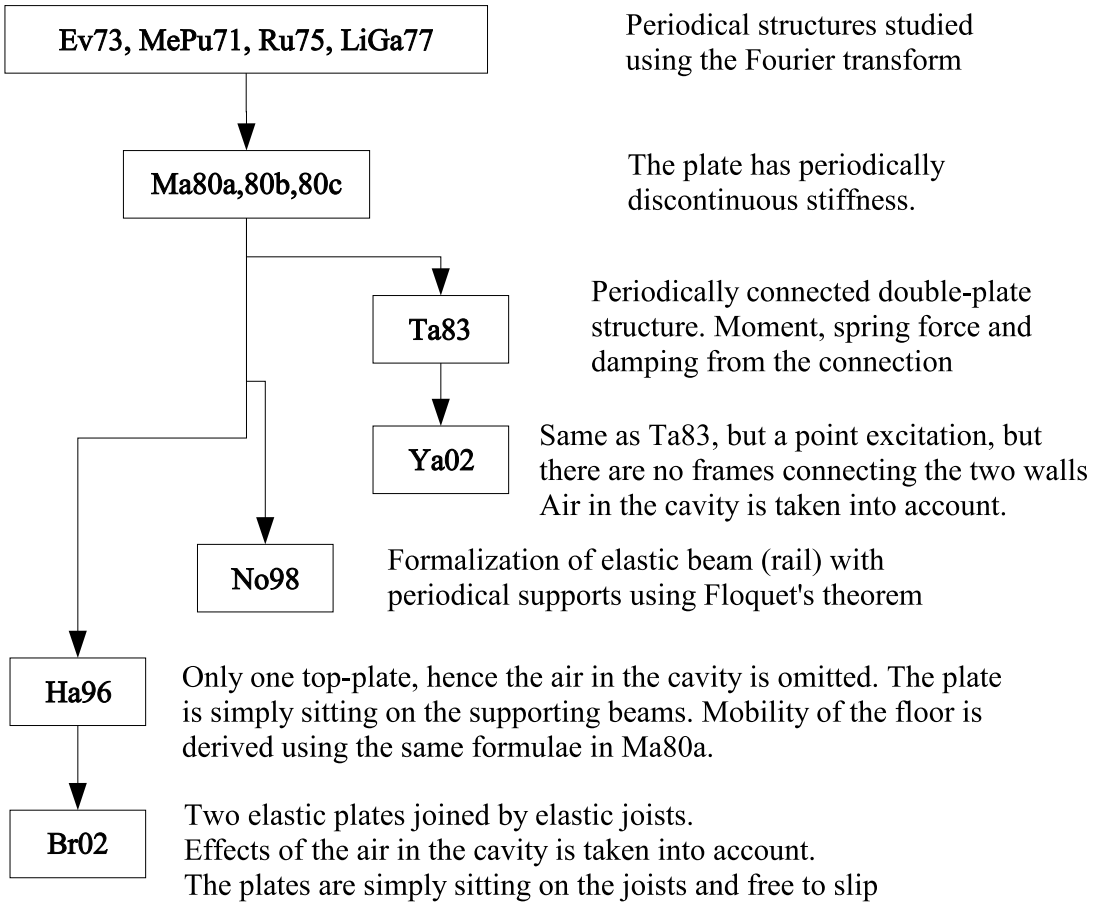

Figure 3-2: group of articles in (a) and brief explanations of them.

Figure 2 shows the papers in Group (a) and short comments describing them. We here mainly discuss the model used by Brunskog Brunskog02, in which a localized time harmonic force is applied on the infinite floor surface. The forcing function is given by

$$F(x, y, t) = \delta(x - x_0, y)e^{i\omega t}$$

where $\delta(x\text{-}x_0,y)$ is Dirac's delta function. The term $\exp(i\omega t\}$ will be omitted since every term is time harmonic. The floor and the ceiling are joined by periodically placed parallel joists (beams). Note that the system is shift invariant in the y-direction, thus the forcing is placed at y=0 (see figure 3-3).

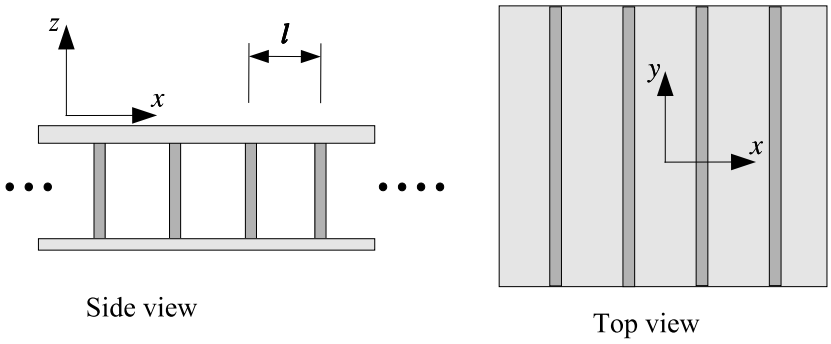

Figure 3-3: Schematic drawing of the model used in Brunskog02.

In Brunskog02, thin plate equations coupled with forces from the air between the plates and the supporting beams (Euler beams)

$$\begin{aligned}\left[D_1\nabla^4_{x\,y} - m_1\omega^2\right] w_1(x,y) &= F + p_c + p_{b1}\\ \left[D_2\nabla^4_{x\,y} - m_2\omega^2\right] w_2(x,y) &= -p_c - p_{b2}\end{aligned} \tag{3-1}$$

where p_a and p_b are the pressure due to the air and the beams between the plates and

$$\nabla^4_{x\,y} = \frac{\partial^4}{\partial x^4} + 2\frac{\partial^4}{\partial x^2 \partial y^2} + \frac{\partial^4}{\partial y^4}.$$

The flexural rigidity of the plate is computed by

$$D = \frac{Eh^3}{12\left(1-\nu^2\right)}$$

where h and v are the thickness of the plate and Poisson's ratio, respectively. In the thin plate theory the thickness h is smaller than other physical dimensions of the plate, such as the span-wise size of the plate and wave length.

Equations (3-1) are equilibrium relationship of the forces in the plates. Δ^2-term (bi-harmonic) and m-term represent the bending and kinetic energy. The external force maybe generated using a tapping machine or human feet, but we do not consider how the force is generated here. When the thin plate theory is used, all displacement components (in-plane and transverse) of the plate surface can be expressed using the vertical displacement of the neutral plane.

A supporting beam is modelled as an Euler beam, which is represented by the following equation

$$\left[EI\frac{d^4}{dy^4} - \sigma\omega^2\right]\eta_n(y) = Q_n,\ -\infty < n < \infty$$

where E, I and σ are the Young's modulus, moment of inertia and the mass density of the beam, respectively. Euler beam is a *1* dimensional version of the thin plate theory, that is, only the bending deformation is taken into account. For an Euler beam $I=bh^3/12$, where b and h are beam's width and thickness, respectively.

There are six unknowns in the system of equations, w_1, w_2, p_c, p_{b1} and p_{b2}. These quantities are related to each other by the following continuity conditions,

$$\begin{aligned} w_1(nl,y) = w_1(nl,y) &= \eta_n(y),\ n = \ldots -2,-1,0,1,2,\ldots\\ p_{b1}(x,y) - p_{b2}(x,y) &= \sum_{n=-\infty}^{\infty} Q_n\delta(x-nl,y).\end{aligned} \tag{3-2}$$

These conditions describe that the beams (joists) and the floor boards are perfectly joined without a gap at all time. However, each component is free to slip as it deforms.

The system of equations is solved using the Fourier transform method, in the (*x,y*)-plane and on the *y*-axis at *x*=*nl*. The Fourier transform of function *w*(*x,y*) in the (*x,y*)-plane is defined as

$$\hat{w}(\alpha,\beta)=\int_{-\infty}^{\infty}\int_{-\infty}^{\infty}w(x,y)\,e^{\mathrm{i}(\alpha x+\beta y)}dxdy.$$

The inverse Fourier transform is then defined as

$$w(x,y)=\frac{1}{(2\pi)^2}\int_{-\infty}^{\infty}\int_{-\infty}^{\infty}\hat{w}(\alpha,\beta)\,e^{-\mathrm{i}(\alpha x+\beta y)}d\alpha d\beta.$$

The Fourier transform of equations (3-1) in the (*x,y*)-plane are

$$\begin{aligned}\left[D_1\left(\alpha^2+\beta^2\right)^2-m_1\omega^2\right]\hat{w}_1(\alpha,\beta)&=\hat{F}(\alpha,\beta)+\hat{p}_{\mathrm{a}}+\hat{p}_{\mathrm{b}1},\\ \left[D_1\left(\alpha^2+\beta^2\right)^2-m_2\omega^2\right]\hat{w}_2(\alpha,\beta)&=-\hat{p}_{\mathrm{a}}-\hat{p}_{\mathrm{b}2},\end{aligned}\tag{3-3}$$

The Fourier transform of on the *y*-axis is

$$\left[K_n\beta^4-\sigma_n\omega^2\right]\eta_n(\beta)=\hat{Q}_n(\beta).\tag{3-4}$$

The Fourier transform of equation (3-2) can be written as

$$\begin{aligned}\hat{p}_{\mathrm{b}1}(\alpha,\beta)-\hat{p}_{\mathrm{b}2}(\alpha,\beta)&=\sum_{n=-\infty}^{\infty}\hat{Q}_n(\beta)\,e^{\mathrm{i}\alpha nl}\\&=\left[K_n\beta^4-\sigma_n\omega^2\right]\sum_{n=-\infty}^{\infty}\eta_n(\beta)\,e^{\mathrm{i}\alpha nl}\end{aligned}$$

Note that we used equation (3-4) and *n*'th supporting beam always remain on the plane, *x*=*nl*. Furthermore, the shear deformation of the beam and the moment acting on the plate result of the shear deformation are excluded from the model.

The system of equation is solved using Poisson's summation theorem,

$$\sum_{n=-\infty}^{\infty}\tilde{w}(nl,\beta)\,e^{\mathrm{i}\alpha nl}=\frac{1}{l}\sum_{n=-\infty}^{\infty}\hat{w}\left(\alpha-\frac{2\pi n}{l},\beta\right),\tag{3-5}$$

where $\hat{w}$ denotes the 1 dimensional Fourier transform of w on the *y*-axis. Because of the above relationship, it is possible to express the transfer function in terms of the summation over the transfer function at $\alpha=2\pi\, n/l$.

The pressure from the air in the cavity can be obtained by solving Helmholtz's equation for the air pressure *p*(*x,y,z*),

$$\nabla^2_{x,y,z}p_{\mathrm{c}}+\frac{\omega^2}{c^2}p_{\mathrm{c}}=0\tag{3-6}$$

with the boundary conditions

$$\left.\frac{\partial p_{\mathrm{c}}}{\partial z}\right|_{z=0}=\omega^2\rho_{\mathrm{c}}w_1,\quad\left.\frac{\partial p_{\mathrm{c}}}{\partial z}\right|_{z=d}=\omega^2\rho_{\mathrm{c}}w_2.$$

Equation (3-6) is then solved using the Fourier transform in the frequency domain.

The pressure from the air outside of the floor system is taken into account in Brunskog02. However, this is omitted here, since the method of solution is the same whether or not the air pressure outside is included.

The techniques in Brunskog02, Yairi02 and Takahashi83 show that any forces (or moments) that can be expressed by linear combinations of w_1 and w_2 can be included in the right hand side of the plate equations (3-1). The equations then can be solved using the same methods given in Brunskog02 and Takahashi83. Furthermore, any linear combinations of the partial derivatives of w_1 and w_2 can also be incorporated in the model.

The model described in this section omits the fact that the floor boards are normally nailed or screwed to the joists. Thus, the movement of the joists and the floor is restricted in some degree. Furthermore, deformation of the floor in the x direction is likely to be influenced by the shear deformation of the joists.

Group (b)

Craik and Smith Craik00 gives detailed studies of the mechanical conditions for double-leaf walls and their frames as a sequel to their preceding paper Craik00a.

In Craik00 the transmission and the reflection of plane waves at the plate-beam (plate-plate) junction is derived from the model explained in Langley90. The transmission is then used in SEA model for the whole wall structure. The wall consists of two plates and frames that connect them. In that regard Craik00 should perhaps be categorized in Group (c). However, we put the paper in Group (b) because it mainly describes the mechanical properties of the plate-beam (or plate) junction. The frames are modelled as either beams or plates. Figure 3-4 gives brief descriptions of the papers in Group (b) and Group (c).

The plate-plate junctions are decomposed into 5 components as shown in figure 3-5. Figure 3-5 shows that all the forces and moments within linear solid mechanics are taken into account to the model. Note that plates 1-4 are semi-infinite, which is different from the model in section 2.1.

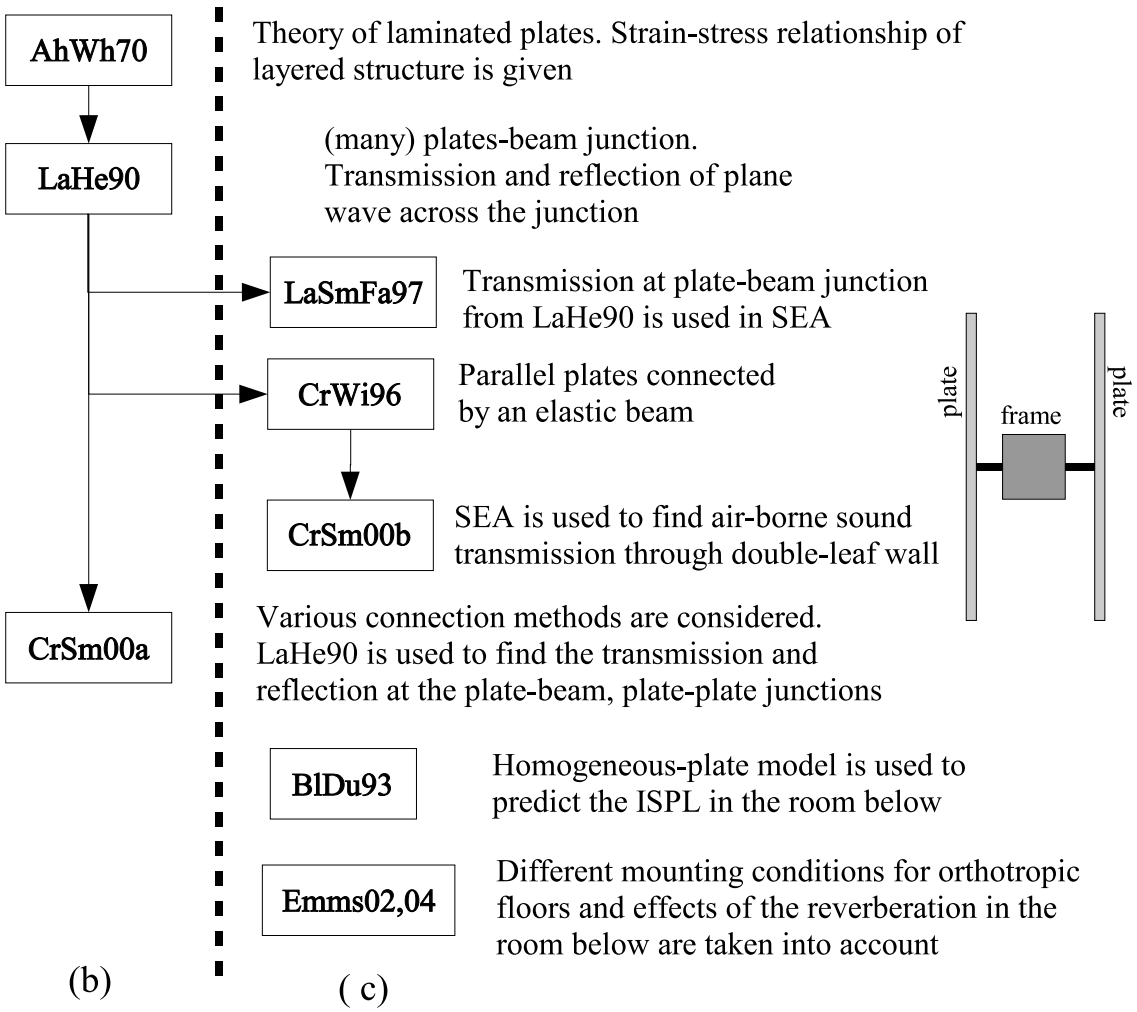

Figure 3-4: The articles in the groups (b) and (c), and brief explanations of them.

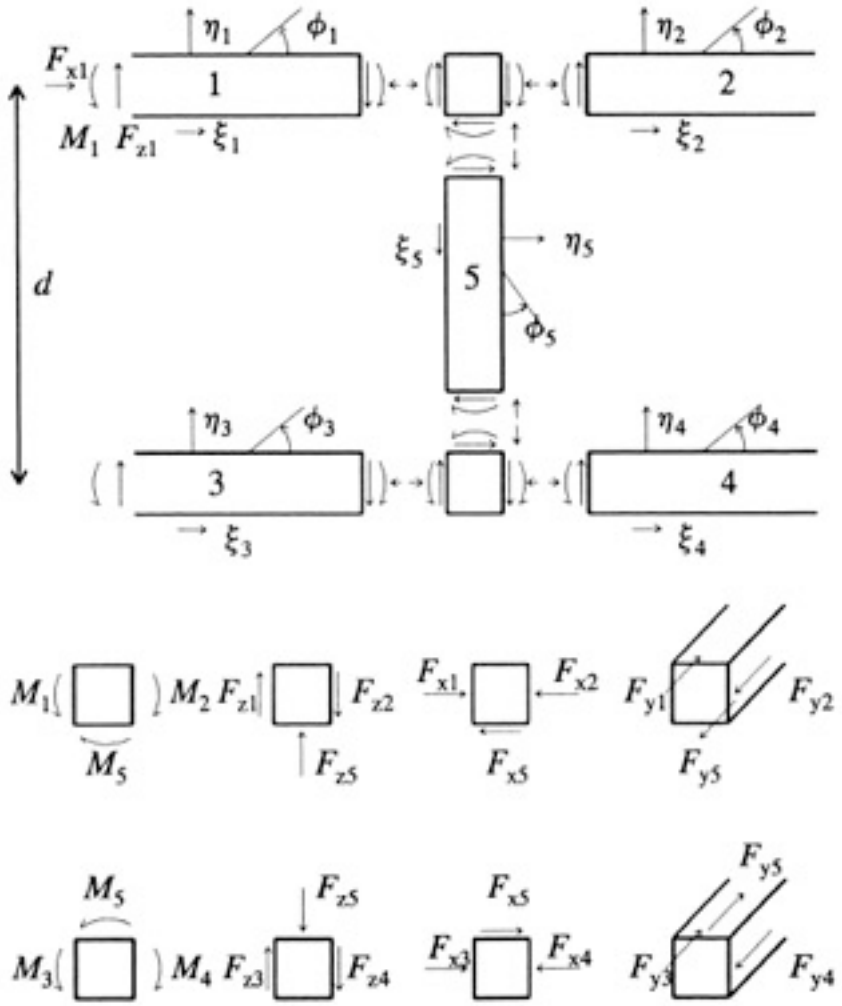

Figure 3-5: Coordinate system, forces and moment acting on each component of the plate-beam junction (copied from Craik00).

In Craik00, it is concluded that the plate-plate junction model performs better than plate-beam model for low-frequency sound. It is not yet confirmed whether or not this is true for wood floors. Plate 1 is excited by a plane wave of frequency ω that is incident from x=-∞ to the junction, then propagates into the rest of the structure. Each plate, for example plate 2, is represented by three displacement components ς_2 (longitudal direction), ζ_2 (longitudal direction orthogonal to ς) and η_2 (transverse direction). Thus, there are five sets of these displacement components for the whole structure.
The equations of motion are

$$\frac{E}{1-\mu^2}\left(\frac{\partial^2\xi}{\partial x^2}+\mu\frac{\partial^2\zeta}{\partial x\partial y}\right)+\frac{E}{2(1+\mu)}\left(\frac{\partial^2\xi}{\partial y^2}+\frac{\partial^2\zeta}{\partial x\partial y}\right)-\rho\frac{\partial^2\xi}{\partial t^2}=0,$$
$$\frac{E}{1-\mu^2}\left(\frac{\partial^2\zeta}{\partial y^2}+\mu\frac{\partial^2\xi}{\partial x\partial y}\right)+\frac{E}{2(1+\mu)}\left(\frac{\partial^2\zeta}{\partial x^2}+\frac{\partial^2\xi}{\partial x\partial y}\right)-\rho\frac{\partial^2\zeta}{\partial t^2}=0,$$

$$\frac{B}{\rho_s}\nabla^4\eta+\frac{\partial^2\eta}{\partial t^2}=0,$$

where ξ and ς are the in-plane displacement and η is the transverse displacement. Note that, there are five plates (see figure 3-5), thus there are five sets of the displacement components.

In contrast to the model in the previous section, the plates here are described using all three independent components of the deformation.

When the plate is excited by a single frequency plane wave incident to the junction at an angle θ, the time and y dependence in the above equations can be taken away. It is also possible to express the waves in each plate by modal expansion. For example plate 1 is expressed by

$$\begin{aligned}\xi_1 = {} & T_{\mathrm{L}0}\cos\theta_{\mathrm{L}0}e^{-\mathrm{i}\,k_{\mathrm{L}0}x\cos\theta_{\mathrm{L}0}} + T_{\mathrm{T}0}\cos\left(\theta_{\mathrm{T}0}+\frac{\pi}{2}\right)e^{-\mathrm{i}\,k_{\mathrm{T}0}x\cos\theta_{\mathrm{T}0}} \\ & + T_{\mathrm{L}1}\cos\theta_{\mathrm{L}1}e^{\mathrm{i}\,k_{\mathrm{L}1}x\cos\theta_{\mathrm{L}1}} + T_{\mathrm{T}1}\cos\left(\theta_{\mathrm{T}1}+\frac{\pi}{2}\right)e^{\mathrm{i}\,k_{\mathrm{T}1}x\cos\theta_{\mathrm{T}1}}\end{aligned}$$

$$\begin{aligned}\zeta_1 = {} & T_{\mathrm{L}0}\sin\theta_{\mathrm{L}0}e^{-\mathrm{i}\,k_{\mathrm{L}0}x\cos\theta_{\mathrm{L}0}} + T_{\mathrm{T}0}\sin\left(\theta_{\mathrm{T}0}+\frac{\pi}{2}\right)e^{-\mathrm{i}\,k_{\mathrm{T}0}x\cos\theta_{\mathrm{T}0}} \\ & + T_{\mathrm{L}1}\sin\theta_{\mathrm{L}1}e^{\mathrm{i}\,k_{\mathrm{L}1}x\cos\theta_{\mathrm{L}1}} + T_{\mathrm{T}1}\sin\left(\theta_{\mathrm{T}1}+\frac{\pi}{2}\right)e^{\mathrm{i}\,k_{\mathrm{T}1}x\cos\theta_{\mathrm{T}1}}\end{aligned}$$

$$\eta_1 = T_{\mathrm{B}0}e^{-\mathrm{i}\,k_{\mathrm{B}0}x\cos\theta_{\mathrm{B}0}} + T_{\mathrm{B}1}e^{-\mathrm{i}\,k_{\mathrm{B}1}x\cos\theta_{\mathrm{B}1}} + T_{\mathrm{n}1}e^{k_{\mathrm{n}1}x}$$

where the bending, longitudal and transverse wave numbers (spatial frequency) are

$$k_{\mathrm{B}} = \sqrt[4]{\frac{\rho_s\omega^2}{B}},\ k_{\mathrm{L}} = \sqrt{\frac{\omega^2\left(1-\mu^2\right)\rho}{E}},\ k_{\mathrm{T}} = \sqrt{\frac{2\omega^2\left(1-\mu^2\right)\rho}{E}}.$$

Note that $T_{\mathrm{T}0}$, $T_{\mathrm{L}0}$ and $T_{\mathrm{B}0}$ are the amplitudes of the incident waves in the two in-plane and transverse (bending waves) directions. The other amplitudes (denoted by T with a subscript) are the unknown amplitudes to be determined. There are oscillatory and exponentially decaying modes in transverse displacement, but only oscillatory modes in the in-plane components. In plates 2 ~ 4, there only the modes that propagate away from the junction I (II). Thus only two modes are needed for the displacement components in plates 2 ~ 4.

The waves travel back and forth between junctions I and II as some energy transmits and some is reflected at the junctions. The displacement components
in plate 5 are

$$\begin{aligned}\xi_5 = {} & T_{\mathrm{L}5+}\cos\theta_{\mathrm{L}5}e^{-\mathrm{i}\,k_{\mathrm{L}5}z\cos\theta_{\mathrm{L}5}} + T_{\mathrm{T}5+}\cos\left(\theta_{\mathrm{T}5}+\frac{\pi}{2}\right)e^{-\mathrm{i}\,k_{\mathrm{T}5}z\cos\theta_{\mathrm{T}5}} \\ & - T_{\mathrm{L}5-}\cos\theta_{\mathrm{L}5}e^{\mathrm{i}\,k_{\mathrm{L}5}z\cos\theta_{\mathrm{L}5}} + T_{\mathrm{T}5-}\cos\left(\theta_{\mathrm{T}5}+\frac{\pi}{2}\right)e^{\mathrm{i}\,k_{\mathrm{T}5}z\cos\theta_{\mathrm{T}5}}\end{aligned}$$

$$\begin{aligned}\zeta_5 = {} & T_{\mathrm{L}5+}\sin\theta_{\mathrm{L}5}e^{-\mathrm{i}\,k_{\mathrm{L}5}z\cos\theta_{\mathrm{L}5}} + T_{\mathrm{T}5+}\sin\left(\theta_{\mathrm{T}5}+\frac{\pi}{2}\right)e^{-\mathrm{i}\,k_{\mathrm{T}5}z\cos\theta_{\mathrm{T}5}} \\ & + T_{\mathrm{L}5-}\sin\theta_{\mathrm{L}5}e^{\mathrm{i}\,k_{\mathrm{L}5}z\cos\theta_{\mathrm{L}5}} + T_{\mathrm{T}5-}\sin\left(\theta_{\mathrm{T}5}+\frac{\pi}{2}\right)e^{\mathrm{i}\,k_{\mathrm{T}5}z\cos\theta_{\mathrm{T}5}}\end{aligned}$$

$$\eta_5 = T_{\mathrm{B}5+}e^{-\mathrm{i}\,k_{\mathrm{B}5}z\cos\theta_{\mathrm{B}5}} + T_{\mathrm{B}5-}e^{\mathrm{i}\,k_{\mathrm{B}5}(z-d)\cos\theta_{\mathrm{B}5}} + T_{\mathrm{n}5+}e^{k_{\mathrm{n}5}z} + T_{\mathrm{n}5-}e^{k_{\mathrm{n}5}(z-d)}$$

where (+) refers to the amplitude of waves travelling from junction I to junction II, (-) refers to the amplitude of waves travelling from junction II to junction I.

The boundary conditions are

$$\begin{aligned}&\eta_1 = \eta_2,\ \eta_1 = -\xi_5,\ \xi_1 = \xi_2,\ \xi_1 = \eta_5,\ \zeta_1 = \zeta_2,\ \zeta_1 = \zeta_5, \\ &\phi_1 = \phi_2,\ \phi_1 = \phi_5,\end{aligned}$$

$$\begin{aligned}&M_1 - M_2 - M_5 = 0, \\ &F_{z_1} - F_{z_2} + F_{z_5} = 0,\ F_{x_1} - F_{x_2} - F_{x_5} = 0,\ F_{y_1} - F_{y_2} - F_{y_5} = 0.\end{aligned}$$

Similarly for the junction II, we have

$$\eta_3 = \eta_4,\ \eta_3 = -\xi_5,\ \xi_3 = \xi_4,\ \xi_3 = \eta_5,\ \zeta_3 = \zeta_4,\ \zeta_3 = \zeta_5,$$
$$\phi_3 = \phi_4,\ \phi_3 = \phi_5,$$

$$M_3 - M_4 + M_5 = 0,$$
$$F_{z_3} - F_{z_4} - F_{z_5} = 0,\ F_{x_3} - F_{x_4} + F_{x_5} = 0,\ F_{y_3} - F_{y_4} + F_{y_5} = 0.$$

The conditions at the junction are then used to determine the coefficients of the modes. The conditions are derived from the equilibrium of the forces and moment. There are 24 unknowns and the same number of equations. In Craik00, the beam is assumed to be either screwed at points or perfectly glued. In the future we may consider modifying the conditions to accommodate some freedom of movement at the contact surface since the floor boards are not normally completely glue to the joists.

In Craik00, it is argued that frame (joists) should be modelled as a plate rather than as a 1 dimensional beam in a low-frequency range. It remains to be seen whether or not an infinite number of periodically placed joists can be modelled (and solved) using the method described in this subsection.

Group (c)

In Emms04, a variational method for an orthotropic plate to find the vertical displacement of the plate that minimizes the total energy in the plate. An orthotropic plate has a constant stiffness in one direction. The total energy in a time interval $[0,t_1]$ is expressed as

$$H\left(w\left(x,y\right)\right) = \int_0^{t_1} L\left(w, \frac{\partial w}{\partial t}\right) dt$$

where L is the Lagrangian of the plate. The formula for L can be found in any of Morse68, Cremer73 and Fahy85. The solution w minimizes H, i.e., the first variation is zero,

$$\delta H\left(w\right) = 0.$$

The solution to the above variational equation can be found numerically using Rayleigh-Ritz method as shown in Emms04.

Sound radiation from a vibrating plate (flat surface at z=0) can be expressed by the following integral over the floor surface

$$p(x,y,z) = -\rho\omega^2 \int_S G\left(x,y,y;x',y',0\right) w\left(x',y'\right) ds'$$

where ρ is the mass density of the air in the room. G denotes Green's function satisfying Neumann condition

$$\left.\frac{\partial G}{\partial n'}\right|_{(x',y',z')\in\partial V} = 0.$$

The walls and the floor of the receiving room are assumed to be acoustically rigid.

Emms Emms04 states that his model does not perform well in the high-frequency range. The model in Blazier94 predicted ISPL using the formula

$$\mathrm{ISPL} = V - f_t - 6 \quad \mathrm{dB}$$

where V and f_t are the maximum velocity of the floor and the transfer function of the floor in dB, respectively.

The total stiffness of the floor structure is calculated using the stiffness of the individual parts and the joint conditions between the plates and the joists from Australian Standard Australia93. It should be noted that the physical parameters used in this model are measured under static forcing on the material. Thus, it is uncertain whether or not those parameters are valid for vibrating structures (with varying frequency).

Concluding remarks

Each of the models introduced here has its strengths and weaknesses. The models in Group (a) give explicit formulae and deformation of the floor everywhere. However, the interaction at the plate-beam junction is overly simplified to exclude any forces acting on the contact surface between the plates and the beams. The models in Group (b) takes into account forces and moment acting on the contacting surface. However, the interaction between the joists is not taken into account. The models in Group (c) can predict the ISPL using the simple formula with the physical parameters of the individual components of the floor. However, the parameters are measured for static load and the model has been shown to be inadequate in predicting the dynamics of the structures.

It is not possible to make a definite statement how well the models shown here predict the performance of real floor structures. Each model lacks some important features of the floor when it is vibrating at a low frequency. There are no standard guidelines how to assess the theoretical models. In order to determine the physical properties of the floor structure, we need to know the details of interaction at plate-joists-plate junctions. Our next step is to compare the models in group (a) with experimental data taken from our own mock-up floor in Tamaki. In the following sections (part II of this chapter), we present our own modelling effort with some comparison between the theory and the experiments.

3.3 PART II: OUR MODELLING FOR LTF FLOOR SYSTEMS

We detail our modelling of the floor/ceiling system in this section. We start with the simplest floor configuration, which consists of the upper plate and the joist beams. The model will then be made more complex to approximate the real experimental structure. The detailed comparison between the theoretical results and the experimental data will be presented in the later chapter. A brief description of the computer codes will also be given at the end of the section.

Solution of a simple joist floor

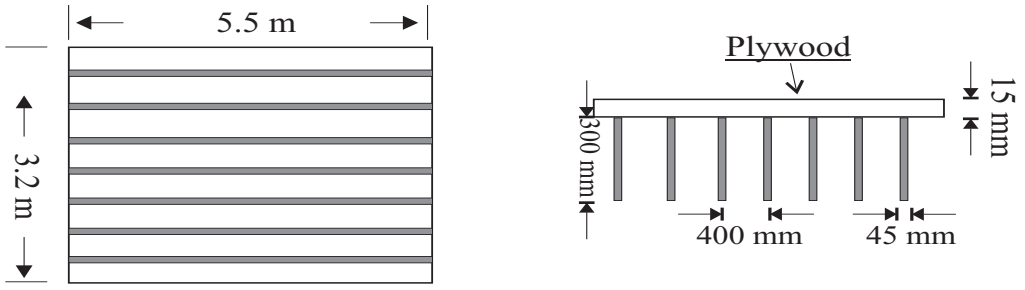

Figure 3-6: Schematic drawing of the experimental mock-up floor.

We consider a joist floor that is spanning over [0,*A*] and [0,*B*] in the *x* and the *y* directions, respectively. The *z*-axis points downward. The thickness of the upper plate and the depth of the

joist are h_0 and h_1, respectively. The cross-section of the structure is shown in figure 3-6. The upper plate is modelled as a Kirchhof plate and the beams are modelled as Euler beams.

Equations for the upper plate and the joist beams

The upper plate is here excited by the time-harmonic forcing with radial frequency ω. The vertical displacement of the plate and the beam, denoted by w_0 and w_1, then satisfies the following plate and beam equations

$$\left[D_0\nabla_{x,y}^4 - m_0\omega^2\right] w_0(x,y) = F\delta(x-x_0, y-y_0) - q_1(x,y) + f_0(x,y), \tag{3-7}$$

where m_0 and F are the mass density per unit area and external force amplitude, respectively. The force from the joists is denoted by P_1. The flexural rigidity, D_0, for the plate is computed by $E_0h_0^3/12(1-\nu^2)$, where E_0 is Young's modulus for the plate.

$$\left[E_1I_1\frac{d^4}{dx^4} - m_1\omega^2\right] w_1(x,j)(x) = q_1(x,j) + f_1(x,j),\ j = 1,2,...,S_1, \tag{3-8}$$

where E_1, I_1 and m_1 are Young's modulus for the beams, moment of inertia and the mass density (per unit length) of the beams, respectively. The moment of inertia is computed by $h_1 d_1/12$, where d_1 is the thickness and the width of the beams. The forces acting on the plate and the beams (on the right hand side of the equation) will be explained in the following subsection.
The differential operator is defined as

$$\nabla_{x,y}^4 = \frac{\partial^4}{\partial x^4} + 2\frac{\partial^4}{\partial x^2\partial y^2} + \frac{\partial^4}{\partial y^4}.$$

Note that the displacement of the beams are denoted by $w_1(x,j)$, $j=1,2,,...,S_1$ for j'th beam.

The above equations can be used for the dynamics of the LTF floor structure in the low frequency range (below 200Hz). In the higher frequency range, the characteristics of the wood change and such a linear model cannot represent the vibrations of the components adequately. Furthermore, the mechanical ambiguity in the structure plays great role in the higher frequency range. Thus the completely deterministic model cannot predict the dynamics of the structure.

Coupling between the floor and the joists

We here consider the coupling between the floor surface and the joist beams. We assume that the two components are linked by springs in the lateral direction along the joist beams. We also assume that the plate and the beams are always in contact. Hence,

$$w_0(x,y_j) = w_1(x,j),\quad j = 1,2,...,S_1, \tag{3-9}$$

where y_j are the locations of the joists.

We consider the elastic resistance between the floor and the joists as they bend then slip as depicted in figure 3-7. The figure describes the discrepancy in the lateral displacement of the floor, which will result in the resisting force at the joining layer. The resistance is assumed to be linear to the length of the slippage, which is determined by the slope of the beam (plate).

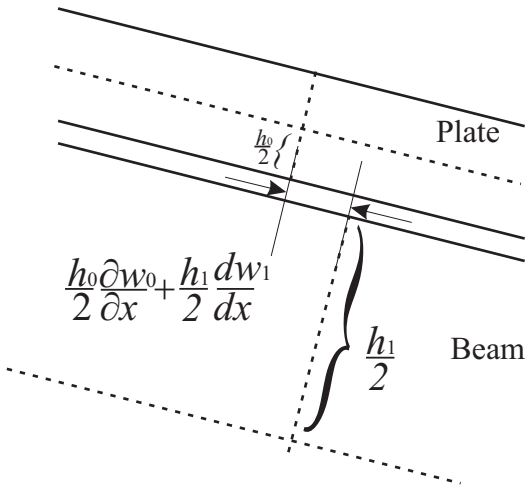

Figure 3-7: Schematic drawing of the cross-section of joining layer (floor-joists). The lateral displacement is given by the sum of the first derivatives of the displacement functions.

The resisting force between the plate and the beam is

$$\sigma\left[\frac{h_0}{2}\frac{\partial}{\partial x}w_0(x,y_j)+\frac{h_1}{2}\frac{d}{dx}w_1(x,j)\right],\quad j=1,2,...,S_1, \tag{3-10}$$

where σ is the spring constant along the joists. The gradient of the floor and the attached joists coincide because of equation (3-9). Hence we have the force acting on the plate and the beam

$$\begin{aligned} f_0(x,y_j) &= \frac{\sigma H h_0}{2}\frac{d^2}{dx^2}w_1(x,j), \\ f_1(x,j) &= \frac{\sigma H h_1}{2}\frac{d^2}{dx^2}w_1(x,j), \end{aligned} \tag{3-11}$$

where $H=(h_0+h_1)/2$. $q_1(x,j)$ denotes the vertical pressure at the contact surface between the upper plate and the j'th joist beam.

The neutral plane of Kirchhoff plates and Euler beams do not stretch. Hence, the structure would not bend when there is no slippage, i.e., $\sigma=\infty$. We here assume that there is always some slippage. The vale σ is will e determined by comparing the theoretical results and the experimental data, which will be shown in later subsection.

Fourier expansion method

The system of equations (3-7)(3-8) with the conditions given by (3-9) and (3-10) can be solved using the Fourier sine-series expansion technique, since the floor and joists are assumed to be simply supported. We show how the coefficients of the expansion can be computed. Note that we use finite number of terms for the expansion because the expansion is intended for numerical computation.

The displacement of the plate and the beams can be expanded as

$$\begin{aligned} w_0(x,y) &= \sum_{m,n=1}^{N} C^0_{mn}\phi_m(x)\psi_n(y), \\ w_1(x,j) &= \sum_{m=1}^{N} C^1_{jm}\phi_m(x), \quad j=1,2,...,S_1, \end{aligned} \tag{3-12}$$

where C_{mn}^{0} C_{jm}^{1} are the unknown coefficient to be determined. The basis functions for the expansion are

$$\phi_m(x) = \sqrt{\frac{2}{A}} \sin k_m x, \quad \psi_n(y) = \sqrt{\frac{2}{B}} \sin \kappa_n y \quad \text{for } m, n = 1, 2, ..., N.$$

The spatial wavenumbers are defined as $k_m = \pi\, m/A$ and $\kappa_n = \pi\, n/B$. These functions satisfy the following orthogonal relationships

$$\int_0^A \phi_m(x)\, \phi_n(x)\, dx = \delta_{mn}, \quad \int_0^B \psi_m(y)\, \psi_n(y)\, dy = \delta_{mn}. \tag{3-13}$$

We now substitute equations (3-12) into (3-7), (3-8) and (3-9), and use the orthogonal relationship given by equation (3-13). The system of equations for the coefficient of the sine-expansion is

$$\begin{aligned} R_{mn}^0 C_{mn}^0 &= F\phi_m(x_0)\,\psi_n(y_0) - \sum_{j=1}^{S_1} \left[\frac{\sigma H h_0}{2} C_{jm}^1 k_m^2 + q_1(m,j) \right] \psi_n(y_j), \\ R_m^1 C_{jm}^1 &= q_1(m,j) - \frac{\sigma H h_1}{2} C_{jm}^1 k_m^2, \; m = 1, 2, ...N. \\ C_{jm}^1 &= \sum_{n=1}^{N} C_{mn}^0 \psi_n(y_j), \; j = 1, 2, ..., S_1. \end{aligned} \tag{3-14}$$

where

$$R_{mn}^0 = D_0 \left(k_m^2 + \kappa_n^2\right)^2 - m_0 \omega^2, \quad R_m^1 = E_1 I_1 k_m^4 - m_1 \omega^2.$$

Equations (3-14) can now be solved numerically.

Description of experiments

The dimension of the experimental joist-floor structure is shown in figure 3-6. An electrodynamic shaker was used to provide a vertical force on the floor upper surface. The shaker was connected to the floor through a wire stinger and a reference force transducer. The shaker body was mounted on a beam that straddled the floor and rested on supports sitting on the concrete collar surrounding the floor. Vibration isolation was provided by very resilient pads. A scanning laser vibrometer (Polytec PSV 300) was used to measure the velocity of the floor normal to the surface. A grid with a spatial resolution of 10-14cm was used to obtain a map of the surface velocity of the floor relative to the input force; both amplitude and phase information was recorded at each frequency. The shaker was driven with pseudorandom signal with a bandwidth from 10 to 500Hz, and a length of 2 seconds (to get a frequency resolution of 0.5Hz). An accelerometer was also placed at the force transducer input to determine the input impedance of the floor.

Computation results

We here compare the theoretical results against the experimental measurements described above. The physical values used in the computation are, m_0 = 0.015x500, m_1 = 0.045x0.3x500, ν = 0.4 and damping ratio for the Young's modulus is 0.04. Two ways of modelling the damping effects are tried here, constant damping coefficient and frequency dependent damping coefficient for the Young's module.

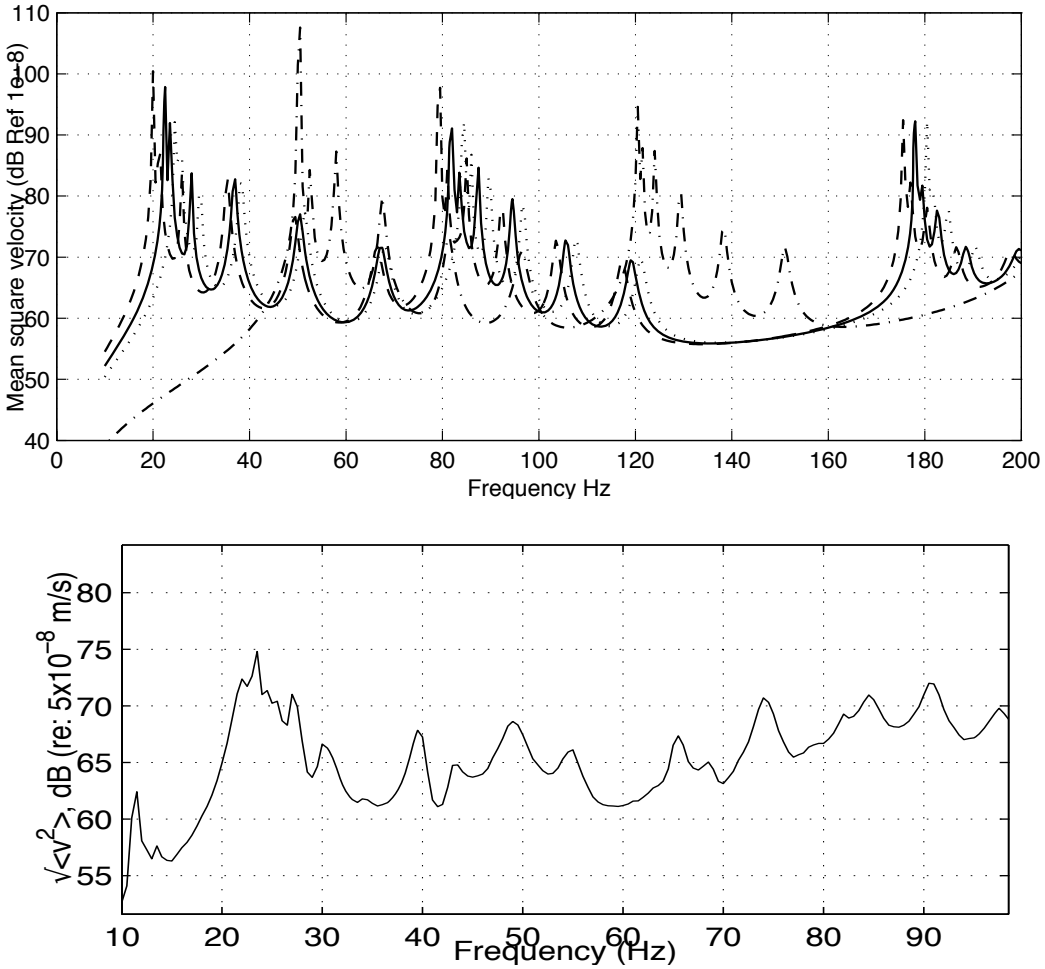

Figure 3-8: Normalized average velocity of the floor surface. (top)Theoretical results for various σ = 0 (dash), 5 * 10^6 (solid), 10^7 (dot) and 10^8 (dash-dot). (bottom) Experimental results.

Figure 3-8 (top) show that the slippage coupling in the model makes substantial difference to the location of the resonance frequencies. As noted in the previous section, the theoretical model breaks down when the resistance, σ, is large.

In a timber structure, the effects of the damping are important. Although, there are many ways to model the damping, however complexity of the damping is outside the scope of this paper. We thus consider the damping as complex valued Young's module. The results in the figures in this section use E_0=10^{10} (1+0.03i)Pa and E_1=1.4x10^9Pa for the joist beams. One may choose frequency dependent damping, that is, the damping ratio is a function of the frequency.

Figure 3-9 shows the measurements of the displacement of the floor surface at frequencies 22Hz, 23.5Hz and 27Hz. The theoretical model on the other hand gives 22.5Hz, 23.5Hz and 28Hz with σ = 5x10^6. The model however overestimates the displacement at the first two resonance frequencies and underestimates at the third resonance frequency. The reason for these discrepancies is yet to be identified.

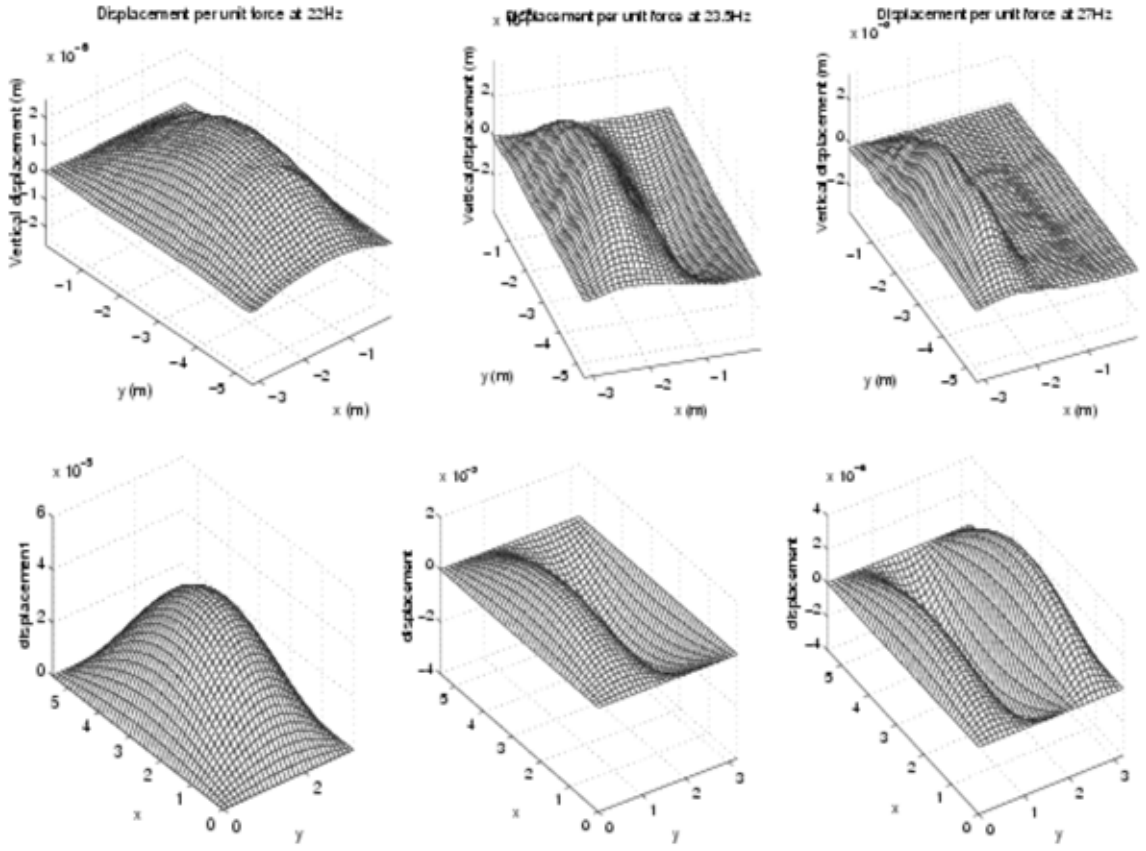

Figure 3-9: Measurements and the theoretical computation of the displacement at the first resonance frequencies. Note that different coordinate orientation is used for the experimental data and the theoretical computation.

Method of solution for multi-layered structures

The Fourier expansion technique shown in the previous sections can be used to find the solutions of structures that are made of more components as depicted in figure 3-10 . We first introduce the notations for the parameters of each component. The layers are denoted by l=0,1,...,M, where the 0'th and the M'th are the upper plate and the ceiling. The layers l=1,2,...,M-1 are the beams that are places perpendicular from one layer to the next. Hence the beams run either in the x or the y direction. The beams are connected by a vertical spring where they meet between the layers, and the spring constant at between the layers l and l+1 is denoted by τ_l, l=1,2,...,M-1.

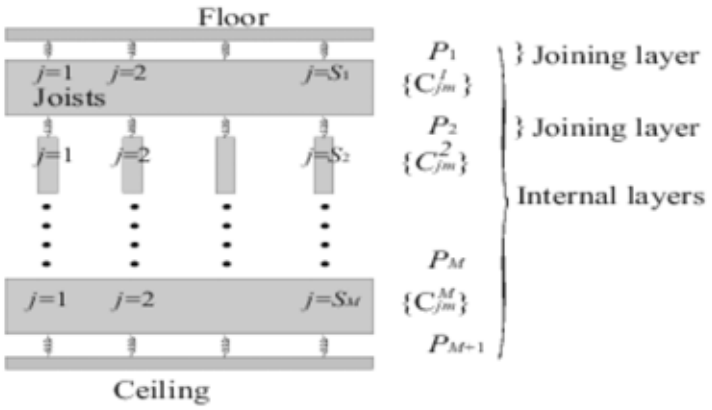

Figure 3-10: Schematic drawing of the cross-section of the floor structure. The origin of the coordinates is placed at the corner of the floor. The z-axis is pointing downwards.

We assume that the same contact conditions exist between the upper plate and the joist beams and the ceiling and the beams. The vertical 1-dimensional springs are used to between the beams in the layers l-1 and l, l=2,3,...,M. The number of beams can be different from a layer to a layer. There is a bottom plate (ceiling), which creates an enclosed cavity. The effects of the air must now be considered.

Equations and Notations

The displacement of the bottom plate, denoted by w_{M+1}, and the beams $w_l(x,j)$, satisfy the following plate and beam equations

$$\begin{aligned} \left[D_M \nabla^4_{x,y} - m_M \omega^2\right] w_M(x,y) &= P_M(x,y) + p(x,y,d), \\ \left[E_l I_l \frac{d^4}{dx^4} - m_l \omega^2\right] w_l(x,j) &= P_l(x,j) - P_{l+1}(x,j), \end{aligned} \tag{3-15}$$

where the notations for the physical parameters follow the same rule given in the previous section. The air pressure on the bottom plate is denoted by $p(x,y,d)$. The air pressure on the top plate is then $p(x,y,0)$.

The pressure between (l-1)'th and l'th layers depends on the difference of the vertical displacement of the beams. Denoting the spring constant by τ_l gives

$$P_l(i,j) = \tau_l \left[w_{l-1}(i,y_j) - w_l(x_i,j)\right], \; i = 1,2,...,S_{l-1}, j = 1,2,...,S_l. \tag{3-16}$$

Hence the right hand side of equation (3-15) is the sum of the above pressures where the beams in (l-1)'th, l'th and (l+1)'th layers.

The acoustic pressure function, $p(x,y,z)$, satisfies the Helmholtz equation

$$\left(\frac{\partial^2}{\partial x^2} + \frac{\partial^2}{\partial y^2} + \frac{\partial^2}{\partial z^2} + \frac{\omega^2}{c^2}\right) p(x,y,z) = 0, \tag{3-17}$$

where c is the speed of sound for the air in the cavity space. This equation is then solved with the boundary conditions (see Cremer73)

$$\left.\frac{\partial p}{\partial z}\right|_{z=0} = \omega^2 \rho w_0, \quad \left.\frac{\partial p}{\partial z}\right|_{z=d} = \omega^2 \rho w_M, \tag{3-18}$$

and the normal derivative of p is zero on the cavity walls, that is, the walls are rigid. The divisions in the cavity by the beams are not considered here. Filling materials in the cavity can be modelled by modifying the parameters c and ω (see Bies and Hansen, 2003).

We here summarize the notations for the solution as there are numerous components in the structure.

$$\begin{aligned} m, n = 1, 2, ..., N &: \text{Number of modes for the Fourier expansion,} \\ l = 0, 1, 2, ..., M &: \text{Number of layers,} \\ j = 1, 2, ..., S_l, &: \text{Number of beams at the } l\text{'th layer,} \\ l = 0,\ l = M &: \text{Indicate the floor and the ceiling} \\ c^l_{jm} &: \text{Coefficients of } j\text{'th beam in } l\text{'th layer,} \end{aligned}$$

Solution for the cavity air

The solution of Helmholtz equation (3-17) can also expressed by the following expansion

$$p(x,y,z) = \sum_{m,n=0}^{N} \xi(z)\,\alpha_m(x)\,\beta_n(y)$$

Where

$$\alpha_m(x) = \cos k_m x,\ \beta_n(y) = \cos \kappa_n y,$$

so that the expansion satisfies the boundary condition at the cavity walls. The unknown function $\xi(z)$ then satisfies the following ordinary differential equation,

$$\frac{\partial^2}{\partial z^2}\xi(z) = \left(k_m^2 + \kappa_n^2 - k^2\right)\zeta(z).$$

Solving the above ordinary differential equation gives,

$$p(x,y,z) = \sum_{m,n=1}^{N} \left\{\Gamma^{(1)}_{mn} e^{\gamma_{mn} z} + \Gamma^{(2)}_{mn} e^{-\gamma_{mn} z}\right\} \phi_m(x)\,\psi_n(y), \tag{3-19}$$

where $\gamma_{mn}=\sqrt{(k^2_m+\kappa^2_n-k^2)}$. The coefficients $\Gamma_{mn}^{(1)}$ and $\Gamma_{mn}^{(2)}$ are to be found from (3-18) and the coupling conditions with other components in the structure.

The boundary conditions (3-18) give the following relationship between the coefficient.

$$\begin{aligned} \rho\omega^2 c^0_{mn} &= \sum{}' \gamma_{mn} \left(\Gamma^{(1)}_{m'n'} - \Gamma^{(2)}_{m'n'}\right) f_A(m,m')\, f_B(n,n'), \\ \rho\omega^2 c^M_{mn} &= \sum{}' \gamma_{mn} \left(\Gamma^{(1)}_{m'n'} e^{\gamma_{m'n'}d} - \Gamma^{(2)}_{m'n'} e^{-\gamma_{m'n'}d}\right) f_A(m,m')\, f_B(n,n'), \end{aligned} \tag{3-20}$$

where

$$\begin{aligned} f_A(m,m') &= \int_0^A \phi_m(x)\,\alpha_{m'}(x)\,dx = \frac{m}{m^2 - m'^2}, \\ f_B(n,n') &= \int_0^B \psi_n(x)\,\beta_{n'}(y)\,dy = \frac{n}{n^2 - n'^2}, \end{aligned}$$

when $m+m'$ ($n+n'$) is odd, otherwise f_A and f_B are zero. Σ' denote the summation over m,n,m',n'.

The effects of the cavity-filling are taken into account using the formulae given in Bies and Hansen.

Derivation of the system of equations for the coefficients

Using (3-21) and (3-22) give

$$
\begin{aligned}
R_{mn}^{0}C_{mn}^{0} &= F\phi_m(x_0)\psi_n(y_0) - \sum{}'\left(\Gamma_{m'n'}^{(1)} + \Gamma_{m'n'}^{(2)}\right) f_A(m,m')\, f_B(n,n') \\
&\quad - \sum_{j=1}^{S_1}\left[q_1(m,j) + \frac{\sigma H h_0}{2} c_{jm}^{1} k_m^2\right]\psi_n(y_j), \\
R_{mn}^{M+1}c_{mn}^{M} &= \sum{}'\left(\Gamma_{m'n'}^{(1)} e^{\gamma_{m'n'}d} + \Gamma_{m'n'}^{(2)} e^{-\gamma_{m'n'}d}\right) f_A(m,m')\, f_B(n,n') \\
&\quad + \sum_{j=1}^{S_M}\left[q_M(m,j) - \frac{\sigma H' h_{M+1}}{2} c_{jm}^{M-1} k_m^2\right]\psi_n(y_j),
\end{aligned}
\tag{3-23}
$$

where $H' = (h_M + h_{M+1})/2$.

The beam equation, using the notations given by (3-16), becomes

$$
R_m^l C_{jm}^l = \sum_{i=1}^{S_{l-1}} P_l(i,j)\,\phi_m(x_i) - \sum_{i=1}^{S_{l+1}} P_{l+1}(i,j)\,\phi_m(x_i).
$$

Equations for the whole structure

We first define the vectors of unknown coefficients in order to formulate the matrix equations for them. The (column) vector notations $\mathbf{C}$, $\mathbf{P}_1$ and $\mathbf{P}_2$ are defined as

$$
\begin{aligned}
\mathbf{C}_a &= (C_{11}^a, C_{12}^a, ..., C_{1N}^a, C_{21}^a, C_{22}^a, ..., C_{NN}^a),\ a = 0, M+1 \\
\mathbf{\Gamma}_a &= \left(\Gamma_{11}^{(a)}, \Gamma_{12}^{(a)}, ..., \Gamma_{1N}^{(a)}, \Gamma_{21}^{(a)}, \Gamma_{22}^{(a)}, ..., \Gamma_{NN}^{(a)}\right),\ a = 1,2, \\
\mathbf{C}_l &= \left(C_{11}^l, C_{12}^l, ..., C_{1N}^l, C_{21}^l, C_{22}^l, ..., C_{S_l N}^l\right),\ l = 2,3,...,M, \\
\mathbf{Q}_1 &= (q_1(1,1), q_1(1,2), ..., q_1(1,S_1), q_1(2,1), q_1(2,2), ..., q_1(N,S_1)), \\
\mathbf{P}_l &= (P_l(1,1), P_l(1,2), ..., P_l(1,S_l), P_l(2,1), P_l(2,2), ..., P_l(S_{l-1},S_l)),\ l = 2,3,...,M, \\
\mathbf{Q}_M &= (q_M(1,1), q_M(1,2), ..., q_M(1,S_M), q_M(2,1), q_M(2,2), ..., q_{M+1}(N,S_M)).
\end{aligned}
$$

The equations for the beams w_l, l=1,2,...M-1, can be expressed by the following system of matrix equations.

$$
\begin{bmatrix}
A^2 & B^2 & C^2 & \cdots & 0 & \cdots \\
0 & A^3 & B^3 & C^3 & & \\
 & & \ddots & & & \\
 & & & \ddots & & \\
\cdots & 0 & \cdots & A^{M-2} & B^{M-2} & C^{M-2}
\end{bmatrix}
\begin{pmatrix} \mathbf{c}^1 \\ \mathbf{c}^2 \\ \vdots \\ \vdots \\ \mathbf{c}^{M-1} \end{pmatrix}
=
\begin{pmatrix} 0 \\ \\ \vdots \\ \vdots \\ 0 \end{pmatrix}
\tag{3-24}
$$

The rows of the above matrix represent the equations that are formulated in the previous subsections. The column vector $\mathbf{c}^l$ is defined from the coefficients of the Fourier expansion of the beam deflection.

The additional equation for the 1'st and the (M-1)'th beams is

$$
\begin{bmatrix}
A^1 & B^1 & 0 & 0 \\
0 & 0 & A^{M-1} & B^{M-1}
\end{bmatrix}
\begin{pmatrix} \mathbf{c}^1 \\ \mathbf{c}^2 \\ \mathbf{c}^{M-2} \\ \mathbf{c}^{M-1} \end{pmatrix}
=
\begin{pmatrix} q_0 \\ q_M \end{pmatrix}
\tag{3-25}
$$

Matrix elements

MatLab codes have been written to directly implement the method of solution given in the previous sections. The codes are written to mimic the real structure as closely as possible, though there are compromises made because of the limitation in the theory. The mock-up floors considered here are built in real size and the surface velocity of the upper plate and the ceiling are measured as described in section 3.

In order to reduce the size of the matrix, the system of equations in section 4 are solved for the coefficients of the upper plate and the ceiling, c^0_{mn}, c^M_{mn}. Hence the size of the matrix is $2N^2$x$2N^2$.

We here give a few examples of the elements of the matrices in equation (3-24).

$$\begin{aligned}
\left[A^1\right]_{((j,m),(j,m'))} &= R^1_m + \tau_1 \sum_{i=1}^{S_2} \phi_{m'}(x_i)\,\phi_m(x_i) + \frac{\sigma H h_1}{2} k^2_m, \\
\left[B^1\right]_{((j,m),(i,n))} &= -\tau_1 \phi_m(x_i)\,\psi_n(y_j),
\end{aligned}$$

for j=1,2,...,S_1.

$$\begin{aligned}
\left[A^2\right]_{((i,n),(j,m))} &= \tau_1 \phi_m(x_i)\,\psi_n(y_j), \\
\left[B^2\right]_{((i,n),(i,n'))} &= -\tau_1 \sum_{j}^{S_1} \psi_{n'}(y_j)\,\psi_n(y_j) - \tau_2 \sum_{j}^{S_3} \psi_{n'}(y_j)\,\psi_n(y_j) - R^2_n, \\
\left[C^2\right]_{((i,n),(j,m))} &= \tau_2 \phi_m(x_i)\,\psi_n(y_j),
\end{aligned}$$

where $[..]_{((i,n),(j,m)),}$ indicates the (i,n)'th row and the (j,m)'th column.

The equations for the coefficients of the upper plate and the ceiling are written into the computer codes in the following form.

$$\begin{bmatrix} R^0 & 0 \\ 0 & R^M \end{bmatrix} \begin{pmatrix} \mathbf{c}^0 \\ \mathbf{c}^M \end{pmatrix} = \begin{pmatrix} \mathbf{F} \\ 0 \end{pmatrix} + \mathcal{T} \begin{pmatrix} \mathbf{\Gamma}^1 \\ \mathbf{\Gamma}^2 \end{pmatrix} + \mathcal{X} \begin{pmatrix} \mathbf{c}^0 \\ \mathbf{c}^M \end{pmatrix}$$

where $\mathcal{T}$ and $\mathcal{X}$ are the matrices derived from equations given in this subsection. R^0 and R^M are the diagonal matrices of $R_m{}^0$ and $R_m{}^M$, respectively.

3.4 MODELLING FIBROUS INFILL

Work has been done by a number of people to predict the effects fibrous materials have on sound propagation, where empirical and physical models have been produced. Bies and Hansen (2003) have produced a summary of aspects of this is their text book. Work by Delaney and Bazley in the late 1960's resulted in an empirical model which was limited in accuracy both by frequency range and by flow resistivity. Bies and Hansen showed an empirical model which tends to the correct limits for both high and low values of $\rho f / R_1$, ρ being the air density, f the frequency and R_1 the flow resistivity. Allard and Champoux have also published an empirical model for sound propagation through fibrous infill, the results of this model are similar to the Bies and Hansen model. These models, however, assumes that the fibrous material is in a rigid frame and hence is not moving with the motion of the air. Unfortunately, if the infill is not backed by some rigid frame it will move with the motion of the air.

Bies and Hansen consider the case of transmission loss through fibrous material. They suggest that if the wavelength of the sound in the fibrous material is longer than ten times the depth of the fibrous material the fibrous material will start to move with the sound waves, resulting in reduced transmission loss through the infill. They provide a graph with which one can estimate the low-frequency transmission loss, based on the flow resistivity.

To our knowledge, there is no effective information about how sound propagates through fibrous infill inside a cavity, given suitable information about the infill (e.g. flow resistivity, density), particularly at low frequencies. Effective models for sound transmission through walls often use some form of empirical model for the effect of the infill in the cavity, given information about the infill[7]. Of course, once such sound transmission models are given information about the acoustic properties of the infill they can work, but the question is how to get these properties from basic knowledge of the infill which is in the cavity.

For the purpose of this project, we will use Bies and Hansen's model to determine the sound propagation through the fibrous infill. Bies and Hansen's model can give us the dimensionless bulk modulus κ and the dimensionless density ρ_m, which are used to calculate the complex speed of sound in the fibrous infill and its complex characteristic impedance. These parameters are functions of the sound frequency and the flow resistivity of the fibrous infill. We will use the experimental results to produce a low-frequency empirical estimate of the infill performance by making the flow-resistivity a function of frequency, producing a kind of rigid-frame equivalent flow resistivity – the flow resistivity the fibrous infill would have had if it had not been moving with the sound waves . We expect that this equivalent flow resistivity will be quite low at very low frequencies and will rise to the normal flow resistivity when the wavelength of sound is less than one tenth of the thickness of the infill.

One way of producing an empirical formulation for what might be called the 'effective' flow resistivity is by a linear interpolation between 0Hz where the transmission loss is apparently zero, and a 'knee' frequency where the transmission loss through fibrous infill starts to level off to a maximum – presumably indicating when the infill is no longer moving significantly with the sound wave. In their textbook, Bies and Hansen have published data showing the transmission loss through fibrous infill at low frequencies. For average flow resistances (400 to 8000 Rayls), we find that this knee frequency occurs when

$$\frac{f\,\rho_B}{R_1} = K\,,$$

where f is the frequency, ρ_B is the density of the fibrous infill, R_1 is the flow resistivity, and K is the knee point constant, which is about 2.
Above this knee point the effective flow resistivity is R_1 , and below this knee point the effective flow resistivity is given by $K\rho_B f$. Note that for this empirical scheme, the important parameter for determining low-frequency effective flow resistivity is the density of the material rather than the flow-resistivity – of course, these two parameters are closely related for a given fibre size.

[7] Ballagh, K., Private correspondence.

3.5 FURTHER COMPARISON OF THE FLOOR MODEL WITH EXPERIMENTAL RESULTS

In this section we look at how the floor model compares with experimental results. We will also use the experimental data to set some parameters, particularly the slipping resistance of the joist to floor upper connection.

Simple floor without ceiling

We first consider the case of a simple floor consisting of 15mm plywood screwed to 300mm deep LVL joists (which are at 400mm centres). The experimental test version of this floor is denoted 'Floor 10'. We use the fundamental frequency and the frequency of the second bending mode along the joist direction to determine the slip resistance; this was found to be about 1.5×10^7 N/m^2. The slipping resistance is not very sensitive to small changes and a 50% change makes little difference. Presumably the slipping resistance is related to the shear stiffness of the plywood and LVL joists as well as slipping between the two layers. The LVL joist Young's modulus was taken to be 14.5GPa. It must be noted that wood stiffness (like all polymers) changes with frequency; higher frequencies give slightly higher stiffnesses. The second resonance frequency from the experimental results gives the dynamic bending stiffness of the plywood along the face grain direction; this was found to be equivalent to a 15mm deep homogeneous plate with a Young's modulus of 12GPa. This can be compared to longitudinal resonance tests of the plywood which showed the along-grain dynamic Young's modulus to be 13GPa. The loss factor of the LVL and the plywood was taken as 0.03.

Figure 3-11 shows the average surface velocity of the experimental and theoretical models using the material properties set out above. They compare well. Differences in the frequency range below 100Hz are due to the panel nature of the plywood causing more complicated modes, giving smaller resonant peaks, whereas the model assumes a continuous layer of plywood. The differences in the frequencies above 100Hz are due to the locally reacting nature of the floor at the forcing point, resulting in large, non-propagating deflections over a small region. These large deflections are difficult to measure properly and so the experimental results may be somewhat inaccurate. Another thing that appears to be happening at frequencies above 100Hz is that the plywood is separating from the joists in the regions between the screws whereas the model assumes a continuous connection.

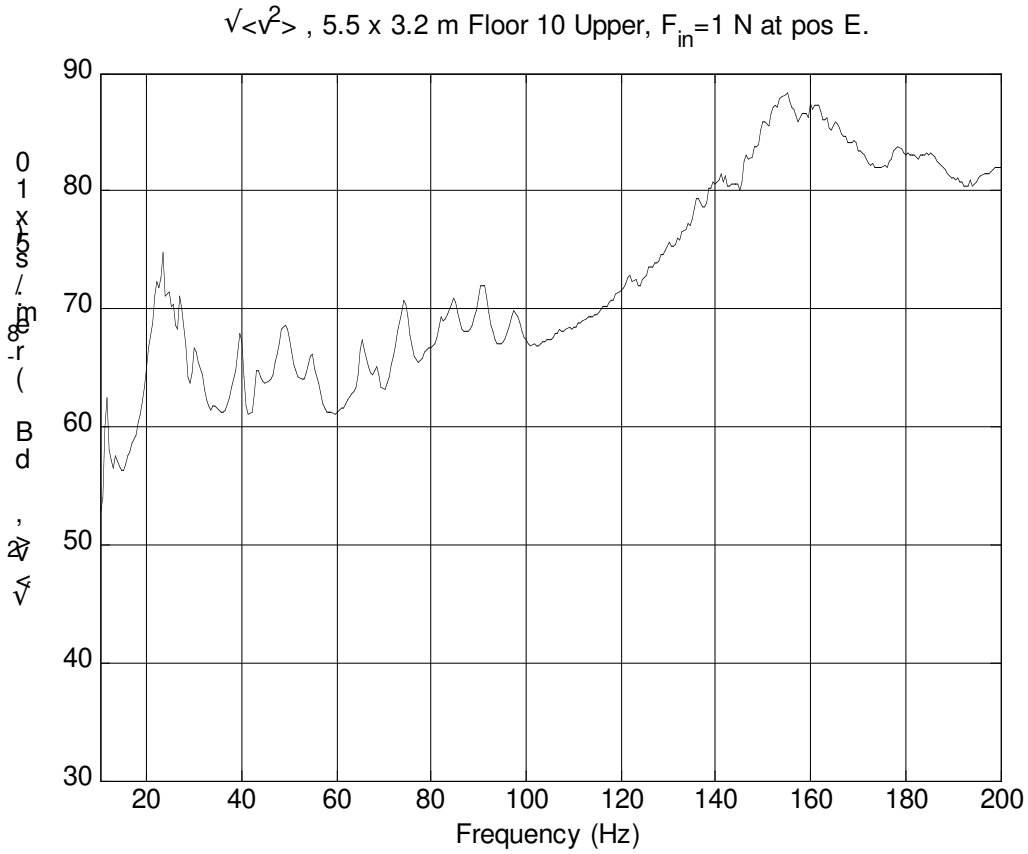

(a)

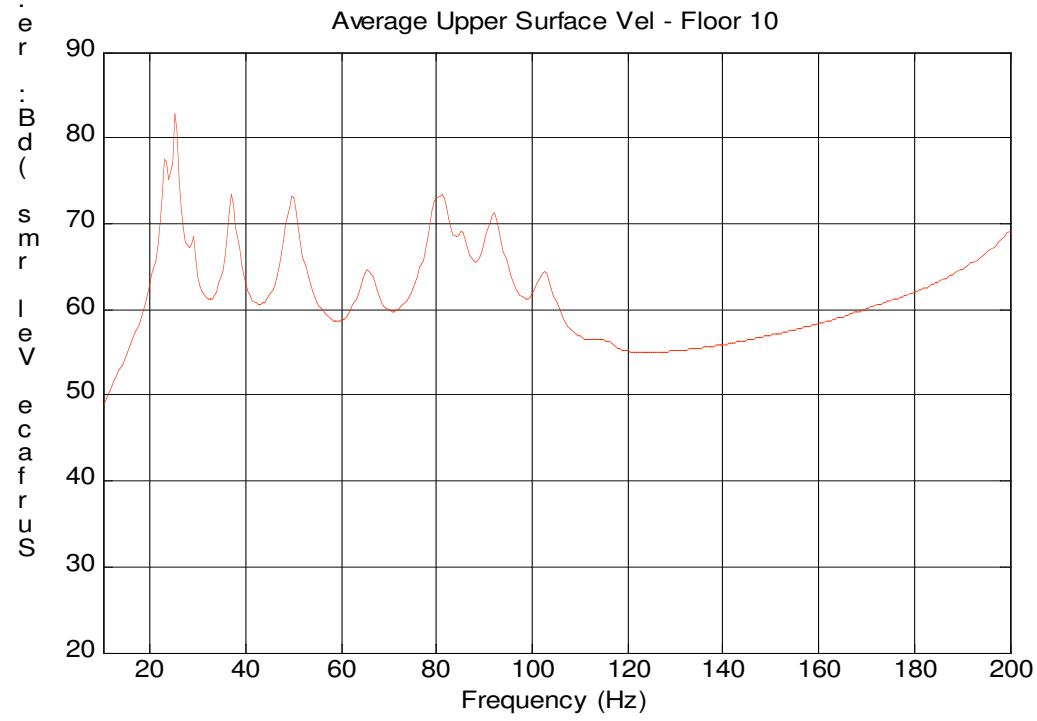

(b)

Figure 3-11. Experimental (a) and theoretical (b) results for the average upper surface velocity of floor 10. The floor is forced vertically at one point on the floor (denoted position 'E' – 0.965m from one side and 1.875m from one end of the floor) and results normalised so that the force has an amplitude of 1N for all frequencies.

Simple floor with plasterboard ceiling on resilient clips

This floor is an extension of the previous floor (as well as being of a different span). It has a ceiling consisting of two layers of 13mm plasterboard screwed to pressed-steel ceiling

battens at 600mm centres, which are attached to every other joist (i.e. at 800mm centres) through resilient clips (RSIC-1 rubber clips). The model assumes that there is a ceiling clip on every joist – this is compensated for by reducing the stiffness of each clip by a suitable amount. The cavity is 358mm deep and is infilled with 2 layers of 150mm sound control type fibreglass batts (Tasman Insulation Midfloor Silencer). The experimental, test version of this floor is denoted 'Floor 10'.

The ceiling battens are Gib Rondo battens 35mm deep and have a calculated stiffness of 11000 Nm^2. The ceiling batten resilient clips have a measured stiffness of 220000 N/m with a 130N constant load, and a loss factor of about 0.1. The infill has a flow resistivity of 7227 Rayls/m and a density of 12 kg/m^3. The plasterboard layers are assumed (through experimental observation) to be slipping and have an isotropic Young's modulus of 3.7 GPa, a density of 962 kg/m^3, and a loss factor of 0.013. For simplicity, the model assumes that the ceiling material stiffness is isotropic, although this is generally not the case.

Figure 3-12 shows the average surface velocity of the ceiling of the experimental and theoretical models using the material properties set out above. They compare well, except for frequencies above 100Hz, where it is suspected that the plywood may be separating from the joists, making the model less valid for this case.

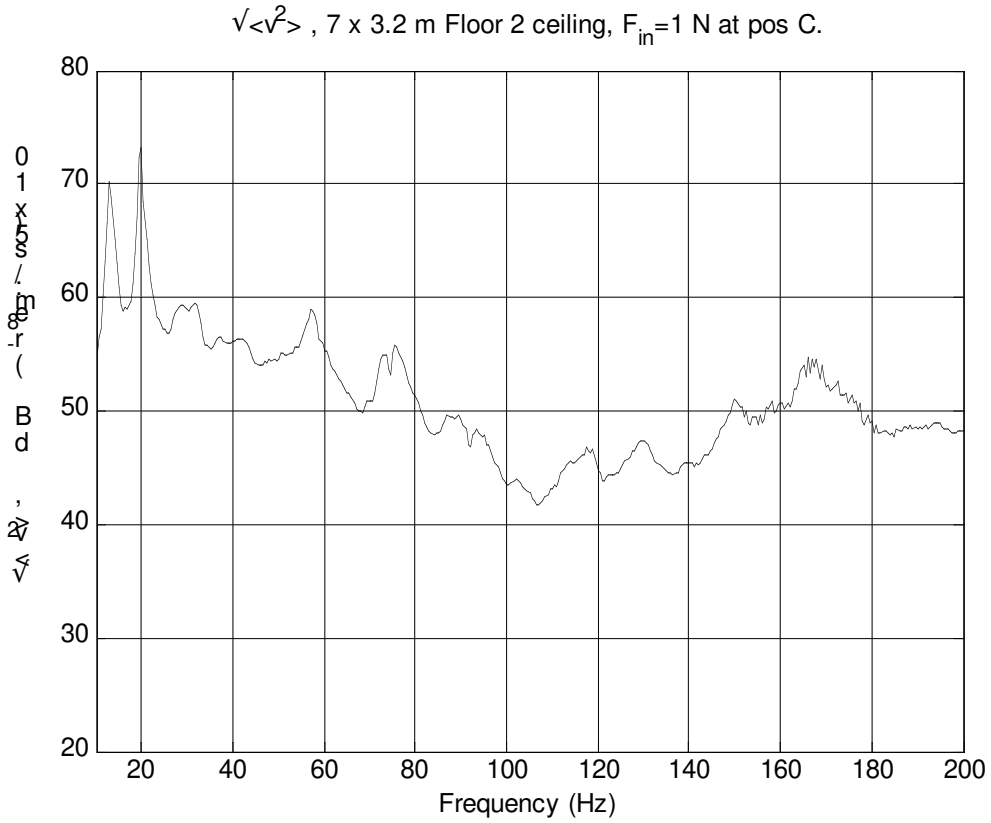

(a)

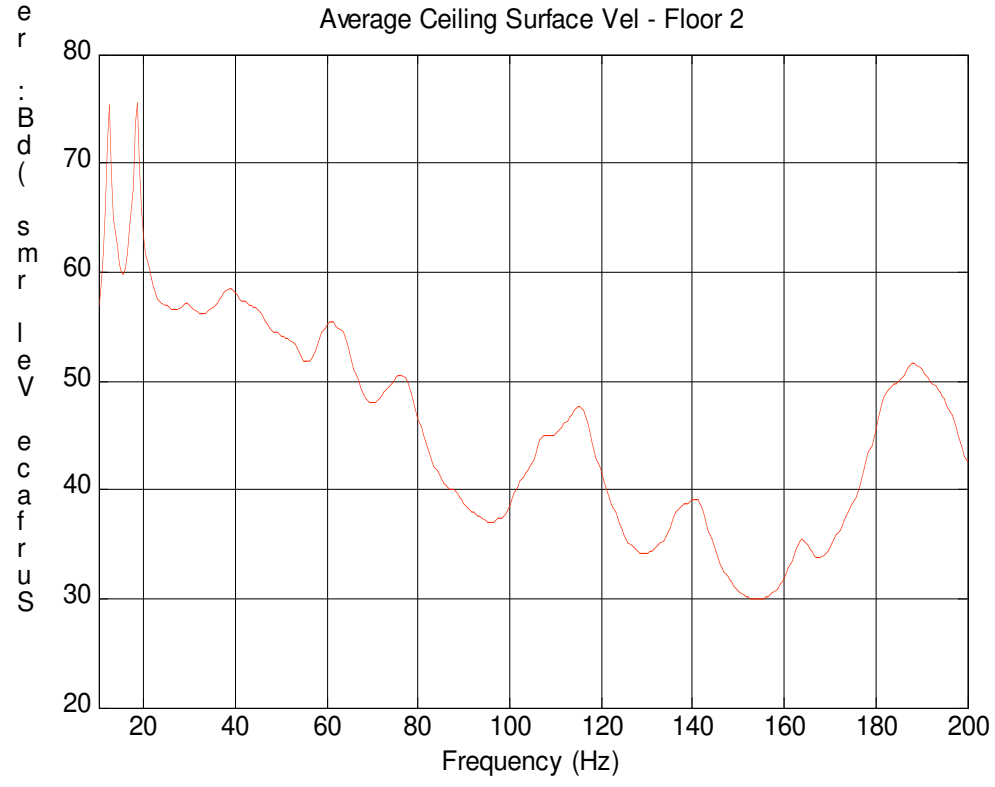

(b)

Figure 3-12. Experimental (a) and theoretical (b) results for the average ceiling velocity of floor 2. The floor is forced vertically at one point on the floor (denoted position 'C' – 0.965m from one side and 2.510m from one end of the floor) and results normalised so that the force has an amplitude of 1N for all frequencies.

Floor with three gypsum fibreboard layers screwed to plywood

This floor is the same as the previous floor (Floor 2), but has three layers of 12.7mm Gib Sound Barrier (a proprietary gypsum fibreboard) screwed to the upper surface of the floor (i.e. the plywood). We compare this floor with the model results to see the effect of having extra stiff layers on the upper surface of the floor.

The gypsum fibreboard is assumed to have a Young's modulus of 4.5GPa, a density of 1040 kg/m^3 and a loss factor of 0.04. The gypsum fibreboard has a reported increased loss factor due to interactions between the layers; in comparison, the material loss factor of the gypsum fibreboard itself is about 0.01. It assumed that the gypsum fibreboard layers are non-slipping and bend together (with the plywood) as one unit.

Figure 3-13 shows the average surface velocity of the ceiling of the experimental and theoretical models using the material properties set out above. They compare well, except for some of the resonances above 100Hz. Exploration with the model shows that these resonances are caused by the ceiling battens; their height is related to the ceiling batten stiffness, and their spacing in frequency due to the ceiling plasterboard properties.

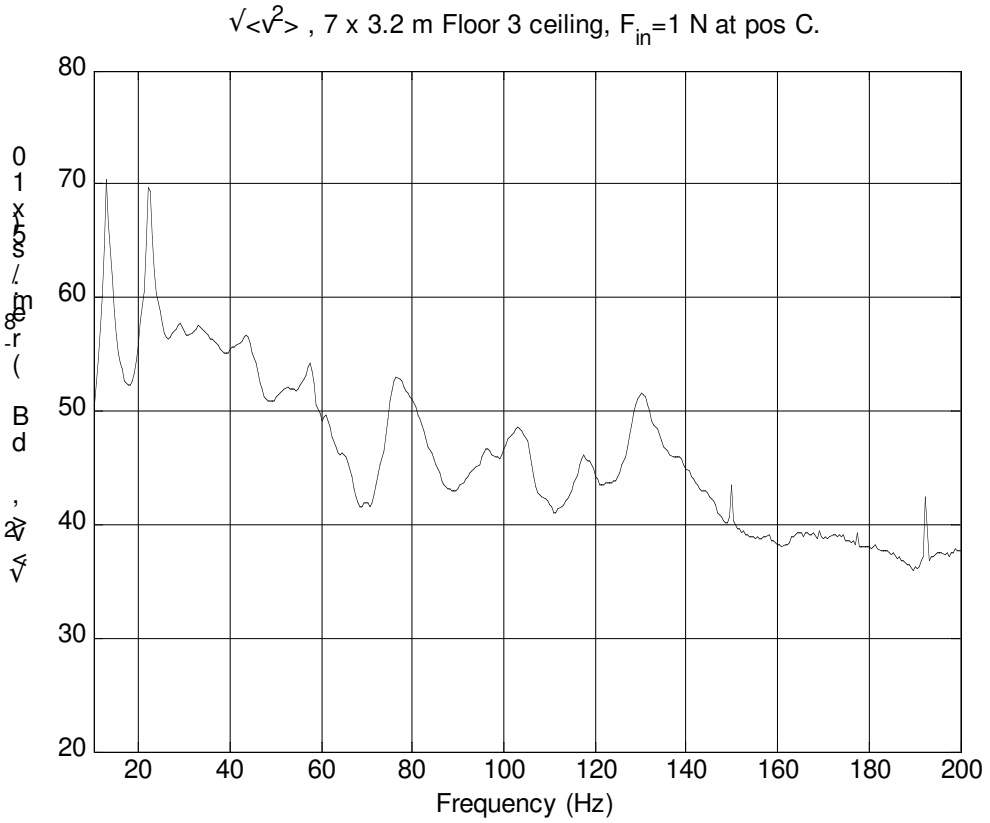

(a)

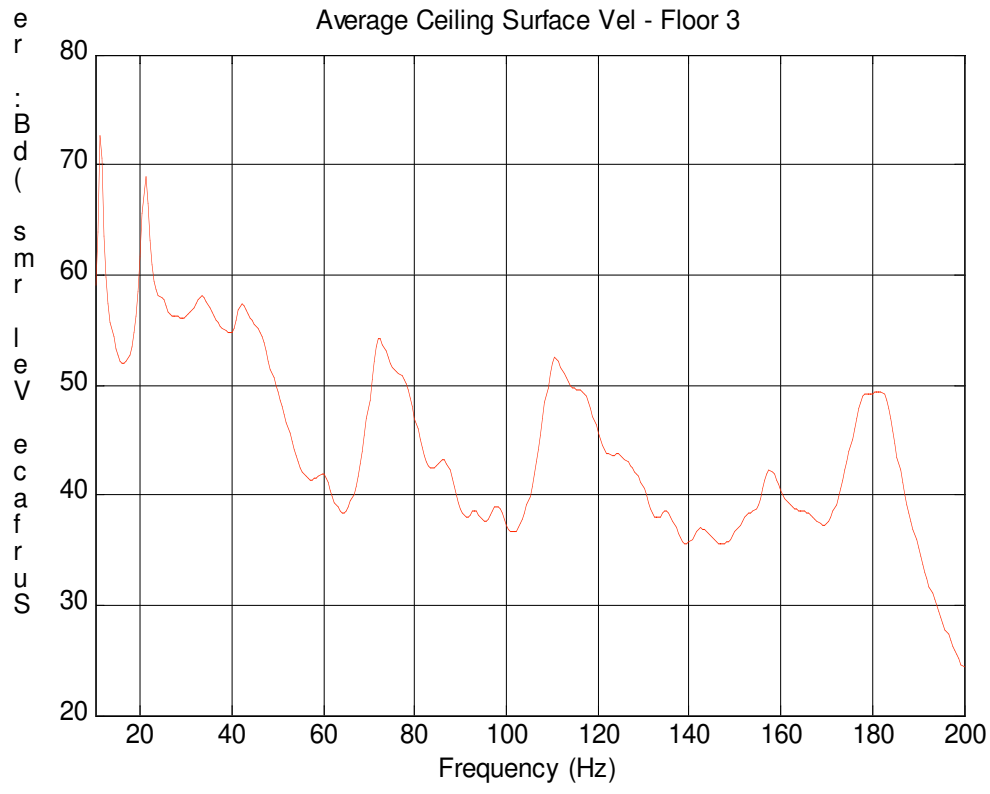

(b)

Figure 3-13. Experimental (a) and theoretical (b) results for the average ceiling velocity of floor 3. The floor is forced vertically at one point on the floor (denoted position 'E' – 0.965m from one side and 1.875m from one end of the floor) and results normalised so that the force has an amplitude of 1N for all frequencies.

Floor with 85mm of sand/sawdust between plywood on upper surface

This floor is the same as Floor 2, but has 90mm deep battens screwed to the upper plywood of the floor (at right angles to the joists) with another layer of plywood on the battens. Between the battens is an 85mm layer of paving sand with sawdust at an 80/20 mix by volume. We compare this floor with the model results to see the effect of having a large amount of mass, stiffness and damping on the upper surface of the floor.

The model is not able to model the upper surface exactly as built, but is able to model an equivalent single upper surface plate with rib stiffeners running perpendicular to the joists. Experimental results (namely the position of the second resonance peak) tell us about the stiffness of this plate. Looking at the decay of the vibrations along the upper surface of the floor we can estimate the loss factor of the upper surface plate (consisting of sand/sawdust and plywood with battens); at 100Hz and above we estimate the loss factor to be between 0.4 and 0.8, at the fundamental resonance we estimated the loss factor to be less than 0.1. Noting from the work of others that the loss factor of sand layers changes with frequency, we assume that the loss factor of the upper floor surface linearly changes from 0 at 0Hz to 0.8 at 200Hz. This is a simplification of a not very well understood phenomenon.

Figure 3-14 shows the average surface velocity of the ceiling of the experimental and theoretical models using the material properties set out above. They compare well, except for some of the resonances between 30 and 50Hz. This is probably due to inaccuracies of the estimated loss factor due to the sand and sawdust fill.

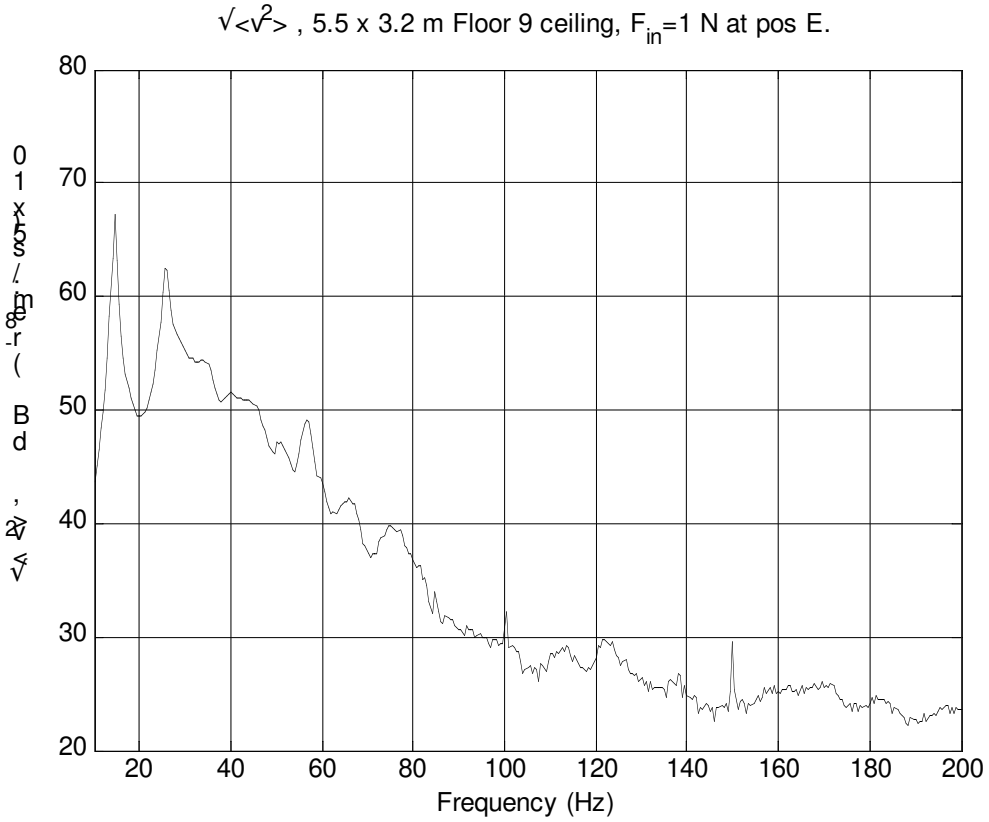

(a)

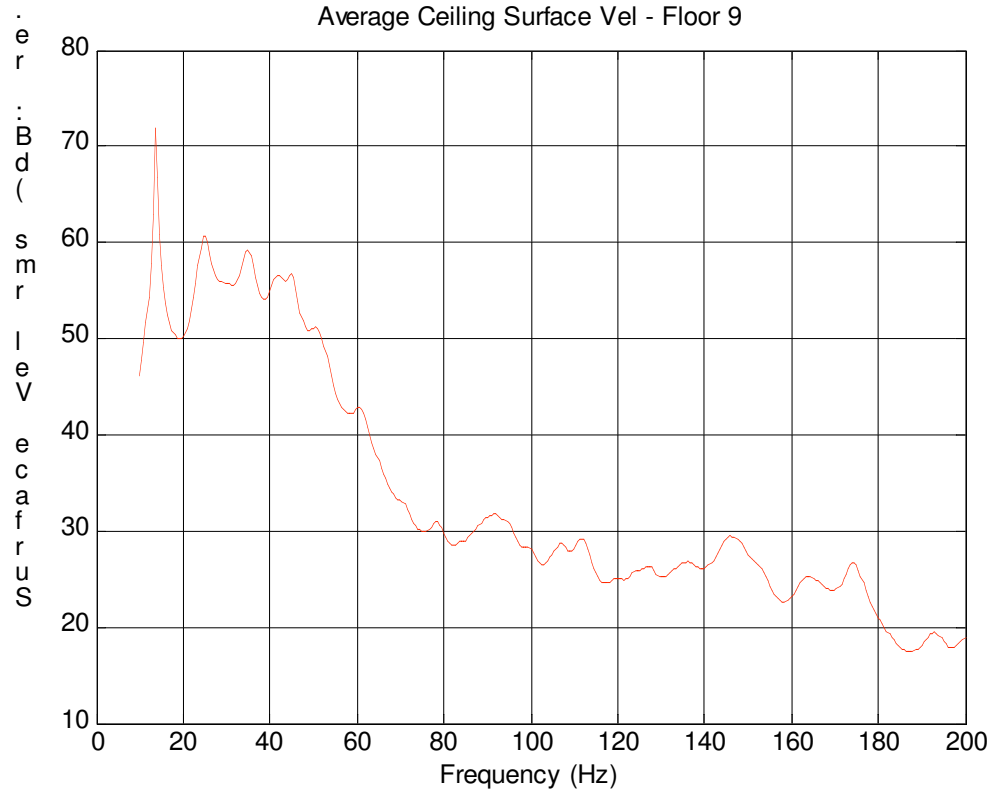

(b)

Figure 3-14. Experimental (a) and theoretical (b) results for the average ceiling velocity of floor 9. The floor is forced vertically at one point on the floor (denoted position 'E' – 0.965m from one side and 1.875m from one end of the floor) and results normalised so that the force has an amplitude of 1N for all frequencies.

Floor with 400mm I-beam joists

This floor has 400mm deep I-beam joists at 600mm centres, with a 20mm particleboard upper surface. It has a ceiling consisting of two layers of 13mm plasterboard screwed to pressed-steel ceiling battens at 600mm centres, which are attached to every other joist (i.e. at 1200mm centres) through resilient clips (RSIC-1). The cavity is 458mm deep and is infilled with 3 layers of 150mm sound control type fibreglass batts (Tasman Insulation Midfloor Silencer). The experimental version of this floor is denoted 'Floor 18'. We compare this floor with the model results to see the effect of having a deeper floor with deep I-beams: deep I-beams have a significant amount of web shear as a component of their deflection performance (around 40% for the 400mm deep I-beams used), whereas the model assumes infinite shear stiffness.

It is assumed that the I-beams have a bending stiffness of 3494000 Nm^2, and the particleboard has a Young's modulus of 4 GPa with a density of 710 kg/m^3.

Figure 3-15 shows the average surface velocity of the ceiling of the experimental and theoretical models using the material properties set out above. They compare well, considering that the model only considers the joists to have a bending stiffness contribution. Resonances are also clearer in the model at the frequencies above 100Hz, suggesting that there is more vibration damping in the real structure than that modelled.

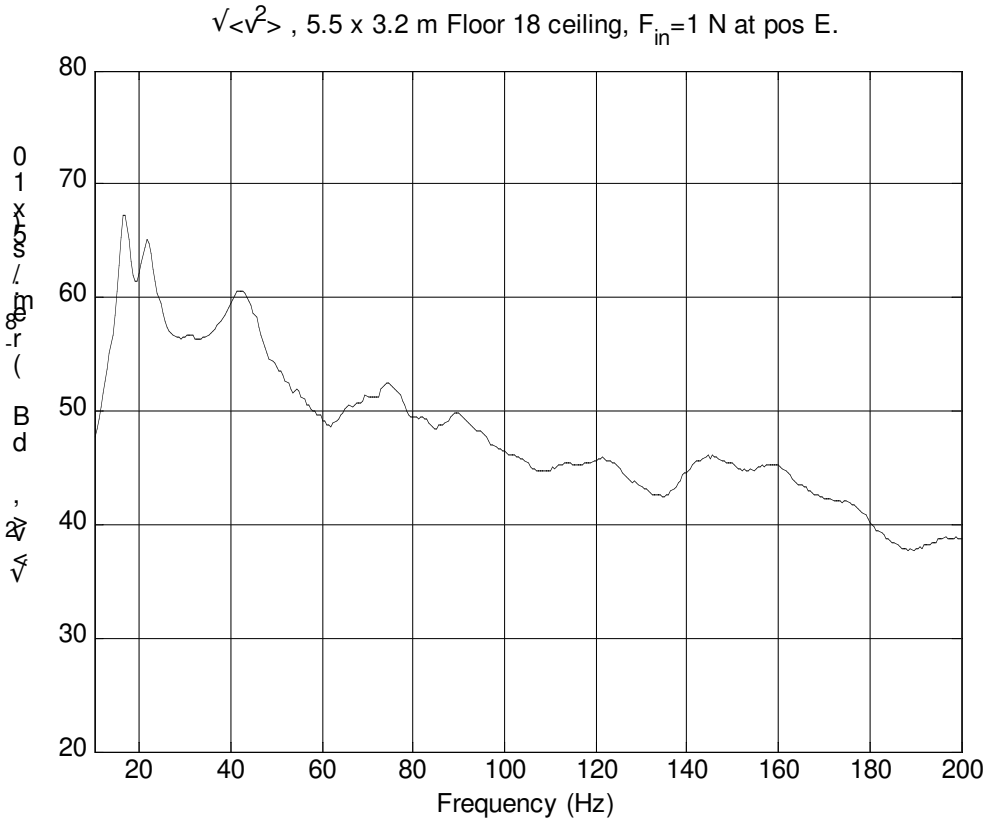

(a)

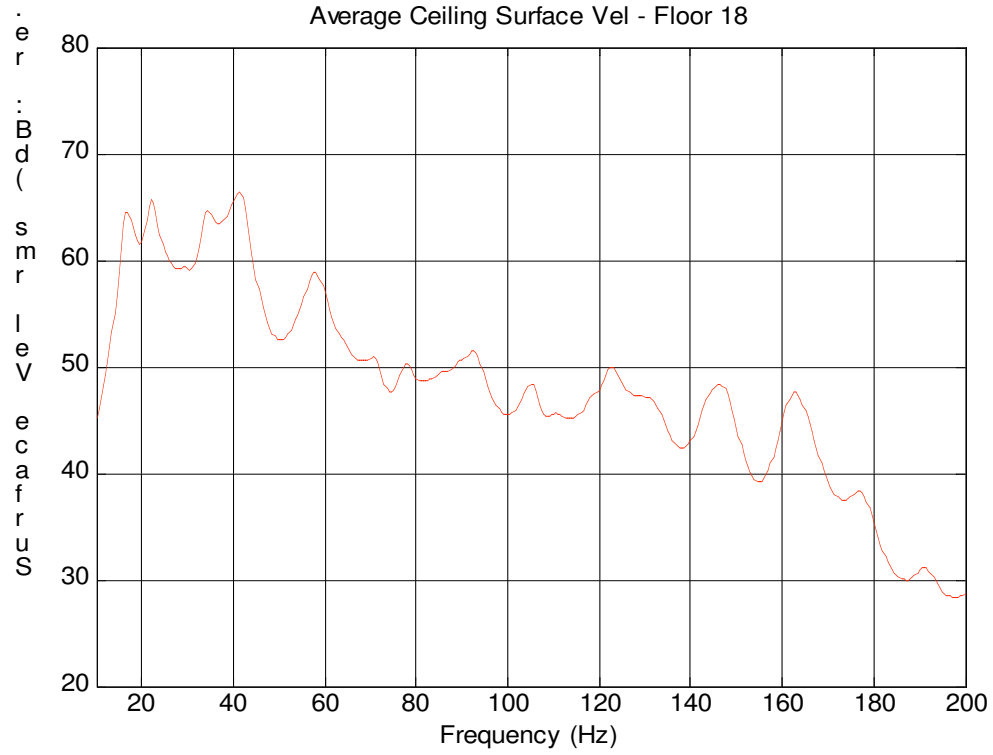

(b)

Figure 3-15. Experimental (a) and theoretical (b) results for the average ceiling velocity of floor 18. The floor is forced vertically at one point on the floor (denoted position 'E' – 0.965m from one side and 1.875m from one end of the floor) and results normalised so that the force has an amplitude of 1N for all frequencies.

General Comments

Overall the model seems to compare well to experiment: it predicts the fundamental and second mode resonances well and follows the general trends correctly, suggesting that using the model to predict overall averages would be quite accurate.

The model can't be an exact comparison because it is a simplified version of the real thing, and because we don't know enough about the parameters of the materials we used for experimental comparison, especially since some properties change with frequency. It could be possible to make a more complicated model which more closely resembles reality. However, such a model would involve having to specify even more material properties, which would be very time consuming to determine.

3.6 PART III: MODELLING THE RECEIVING ROOM

One of the important aspects of low-frequency sound transmission is the effect of the receiving room on the sound generated by the vibrating floor/ceiling system. There is a reasonable amount of literature on the subject of how room size and dimension affects performance of airborne sound transmission through walls, but not a lot about impact sound transmission through floors. For our purposes, we would like to predict the sound pressure generated by the vibrating ceiling in the room below; one aim would be to find the average sound pressure in this so-called receiving room. We note that many researchers assume an infinitely-sized room and essentially look at the sound power radiated by the ceiling. This infinitely large room approach does not consider the effects the resonances in the room have on the sound pressure generated by the vibrating ceiling; this approach also does not consider the effects near-field radiation might have. For example, even vibrating modes do not generate much radiated sound power in an infinitely-sized room, but nearer to the ceiling there is a lot sloshing of air backwards and forwards between peaks and troughs in the ceiling vibration, and this must contribute to the sound pressure detected in the receiving room.

Although not much exists on this subject, it is not difficult to predict the sound pressure generated in a room by a vibrating ceiling if one makes suitable approximations. We basically assume that the room is a rectangular box with a uniform absorption of sound energy over its surface.

The theory

The theory of the room is based on work published by Morse and Ingard (1986,section 9.4).

For a ceiling with surface displacement $w(x', y')$ vibrating at frequency ω, the sound pressure in the room below is given by

$$p_{rec}(x, y, z) = -\rho\omega^2 \iint_{l_x l_y} G(x, y, z \mid x', y') w(x', y') dS' ,$$

where x, y and z is a point in the room, l_x and l_y are the dimensions of the floor, ρ is the air density, and S' is the ceiling surface with x' and y' being location of a point on the ceiling. G is the Green's function which describes the propagation in the room as is given by

$$G(x, y, z) = \sum_{n_x n_y n_z}^{\infty} \frac{\cos\left(\frac{\pi n_x x}{l_x}\right)\cos\left(\frac{\pi n_y y}{l_y}\right)\cos\left(\frac{\pi n_z z}{l_z}\right)\cos\left(\frac{\pi n_{x'} x'}{l_{x'}}\right)\cos\left(\frac{\pi n_{y'} y'}{l_{y'}}\right)}{V \Gamma_n (k_n^2 - k^2 - i\tau_n)},$$

where n_x, n_y and n_z are the mode numbers of the room in the x, y and z directions respectively (n being a short form of this i.e. $n = \{n_x, n_y, n_z\}$), V is the room volume, k is the wavenumber.

Also

$$k_n^2 = k_{nx}^2 + k_{ny}^2 + k_{nz}^2 \quad ; k_{nx} = \frac{\pi n_x}{l_x}, k_{ny} = \frac{\pi n_y}{l_y}, k_{nz} = \frac{\pi n_z}{l_z},$$

$$\tau_n = k\left[\varepsilon_{nx}\left(\frac{\beta_{x0}+\beta_{xl}}{l_x}\right) + \varepsilon_{nx}\left(\frac{\beta_{y0}+\beta_{yl}}{l_y}\right) + \varepsilon_{nx}\left(\frac{\beta_{z0}+\beta_{zl}}{l_z}\right)\right],$$

$$\Gamma_n = \frac{1}{\varepsilon_{nx}\varepsilon_{ny}\varepsilon_{nz}}$$

where the β's are the surface admittances on each of the six surfaces of the room, and

$$\varepsilon_{nx} = \begin{cases} 1 & , n_x = 0 \\ 2 & , n_x > 0 \end{cases}, \quad \varepsilon_{ny} = \begin{cases} 1 & , n_y = 0 \\ 2 & , n_y > 0 \end{cases}, \quad \varepsilon_{nz} = \begin{cases} 1 & , n_z = 0 \\ 2 & , n_z > 0 \end{cases}.$$

To simplify things, we assume that the surface admittance is the same on all surfaces. For random incidence of sound we can also assume that the surface admittance and the absorption coefficient of the room surfaces are related by (Morse and Ingard, 1986, p 580)

$$\alpha = 8\,\mathrm{Re}\{\beta\}.$$

We can use the above formulation to calculate the sound pressure inside the room, and by selecting a large number of points (typically several hundred) and averaging them, we can find the average sound pressure inside the receiving room.

Testing the receiving room model

There are a number of ways to confirm the accuracy of the theory and resulting code: you can examine the low-frequency limits in the room, and you can model a monopole at the corner of the floor for a number of limiting situations. These were done to confirm that the model works.

One can also compare prediction to measurement for the sound pressure generated by a floor on a room. This was done for a rectangular room measuring 3.2m by 3.6m by 3.05m high. It had plasterboard walls and a concrete floor. The floor also measured 3.2m by 3.6m, and was particleboard type floor. The vibration of the underside of the floor was measured by accelerometers in a grid patterns with a resolution of 200mm. The resulting accelerations where normalised against the force produced by an excitation hammer (including phase information). Inside the room the sound pressure was measured by microphone at 25 measurement points across the volume of the room. Figure 3-16 shows the resulting comparison of measured average sound pressure in the room and the sound pressure predicted by the model using the measured vibrations of the underside of the floor above the room. The absorption coefficient of the room was assumed to be 0.15 for the model, based on work by Maluski and Gibbs (2004), and 200 random points were averaged inside the model room. There is a good correspondence between the model and the measurement, considering that relatively few sound pressure measurement points were used inside the room. We also must realise that the model is a sort of ideal room and no real room matches it exactly, but at low frequencies there is a good correspondence at we are able to use it to indicate what is likely to happen in a real room.

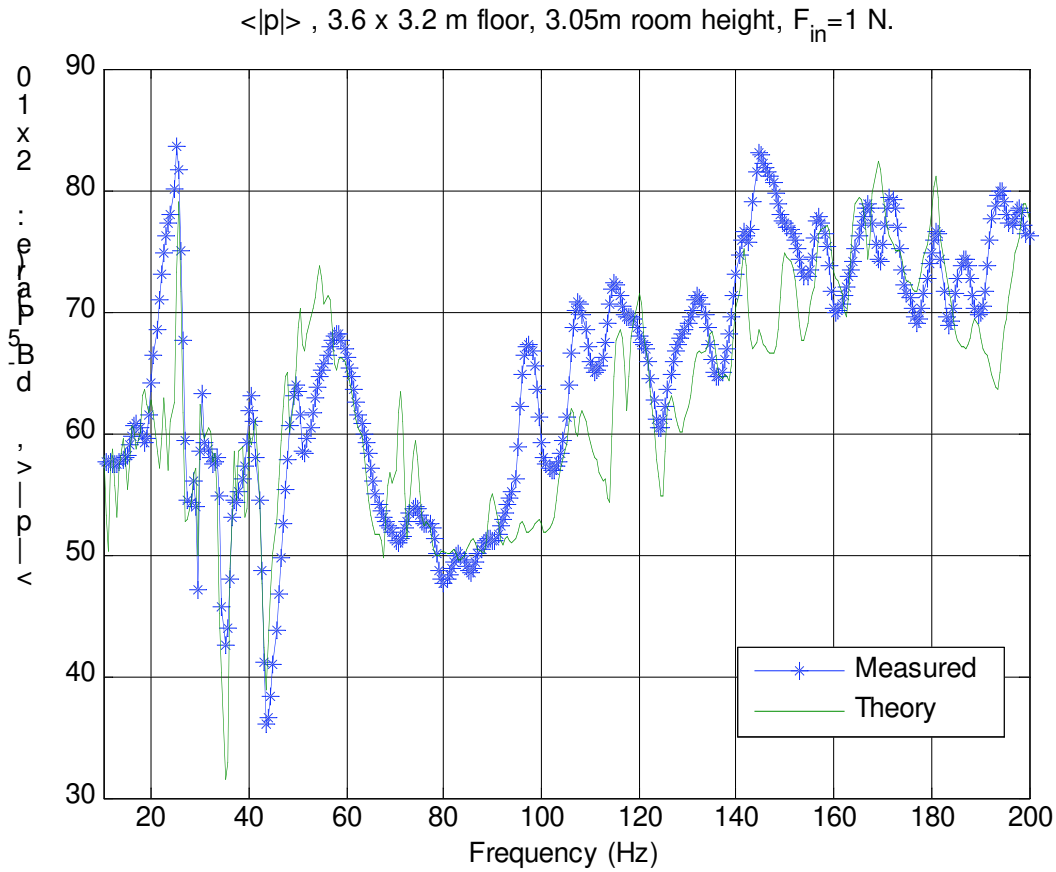

Figure 3-16. Prediction and measurement of the average pressure in a receiving room.

3.7 REFERENCES

Allard, J-F, Champoux, Y., (1992). New empirical equations for sound propagation in rigid frame fibrous materials, J. Acoust. Soc. Am. 91 (6).

Ashton, J.E. and Whitney, J.M. (1970), *Theory of Laminated Plates*, Technomic Publishing Co, Stamford, Conn.

Australian Standard, Standard Australia, 1993.

Bies, D.A. and Hansen, C.H. (1988) *Engineering Noise Control, Theory and practice*, Unwin Hyman Ltd., London

Bies, D. A. and Hansen, C. H., (2003). Engineering Noise Control: Theory and Practice, 3rd Edition.

Blazier, W.E. and DuPree, R.B. (1994) "Investigation of low-frequency footfall noise in wood-frame, multifamily building construction", *J. Acoust. Soc. Am.*, 96, pp. 1521--1532.

Brunskog, J. (2002) *Acoustic Excitation and Transmission of Lightweight Structures*, PhD thesis, Lund University.

Craik, R.J.M. and Smith, R.S. (2000) "Sound transmission through double leaf lightweight partitions part {I}: Airborne sound", *Applied Acoustics*, 61, pp. 223--245.

Craik, R.J.M. and Smith, R.S. (2000) “Sound transmission through lightweight parallel plate. part {II}: Structure-brone sound”, *Applied Acoustics*, 61, pp. 247--269.

Craik, R.J.M. and Wilson, R. (1996), “Sound transmission through parallel plates coupled along a line”, *Applied Acoustics*, 49, pp. 353--372.

Cremer, L. Heckl, M. and Ungar, E. (1973) *Structure-Borne Sound*, Springer-Verlag, New York.

Emms, G (2004) “The effect of mounting conditions on low-frequency impact sound insulation of timber floors”, ICA porceedings, April.

Emms, G. and Hollows, R. (2002) “Using sound intensity to measure the impact insulation of floors”, in *The 2002 International Congress and Exposition on Noise Control Engineering*, August.

Evseev, V.N. (1973) “Sound radiation from an infinite plate with periodic inhomogeneities”, *Soviet Physics Acoustics*, 19, pp. 345--351.

Fahy,F.S. (1985) *Sound and Structural Vibration*, Academic Press Ltd., London.

Hammer, P. (1996) “Vibration isolation on light weight floor structures”, *Tech. Report* TVBA-3078, Department of Engineering Acoustics, Lund University.

Langley, R.S. and Heron, K.H. (1990) “Elastic wave transmission through plate/beam junctions”, *Journal of Sound and Vibrations*, 143, pp. 241--253.

Langley, R.S. Smith, J.R.D. and Fahy, F.J. (1997) “Statistical energy analysis of periodically stiffened damped plate structures”, J. Sound and Vibration, 208, pp. 407--426.

Lin, G. and Garrelick, J.M. (1977) “Sound transmission through periodically framed parallel plates”, *J. Acoust. Soc. Am.*, 61, pp. 1014--1018.

Mace, B.R. (1980) “Sound radiation from a plate reinforced by two sets of parallel stiffeners”, *Journal of Sound and Vibration*, 71, pp. 435--441.

Mace, B.R. (1980) “Periodically stiffened fluid-loaded plates, {I}: Response to convected harmonic pressure and free wave propagation”, *Journal of Sound and Vibration*, 73, pp. 473--486.

Mace, B.R. (1980) “Periodically stiffened fluid-loaded plate, {II}: Response to line and point forces”, *Journal of Sound and Vibration*, 73, pp. 487--504.

Maluski, S., Gibbs, B.M. (2004). “The effect of construction material, contents and room geometry on the sound field in dwellings at low frequencies,” *Applied Acoustics*, 65, pp 31-44.

Mead, D.J. and Pujara, K.K. (1971) “Space-harmonic analysis of periodically supported beams: Response to convected random loading”, *Journal of sound and vibration*, 14, pp. 525--541.

Morse, P. and Ingard, K. (1968) *Theoretical Acoustics*, McGraw-Hill, New York.

Morse, P.M., Ingard, K.U. (1986), *Theoretical Acoustics*, Princeton University Press. Section 9.4.

Rumerman, M (1975) "Vibration and wave propagation in ribbed plates", *J. Acoust. Soc. Am.*, 57, pp. 370--373.

Takahashi, D. (1983) "Sound radiation from periodically connected double-plate structures", *Journal of Sound and Vibration*, 90, pp.541--557.

Yairi, M., Sakagami, K., Sakagami, E., Morimoto, M., Minemura, A. and Andow, K. (2002) "Sound radiation from a double-leaf elastic plate with a point force excitation: Effect of an interior panel on the structure-borne sound radiation", *Applied Acoustics*, 63, pp. 737--757.

Zaher, A. (2004) "Development of a wooden joist floor with high impact sound insulation", *Tech. Report, Acoustics Research Centre*, The University of Auckland.